PERMANENT MAGNET ALTERNATOR CONTROL BY MEANS OF MAGNETIC SATURATION

WILLIAM L. AITKENHEAD
AND
FRANK C. ANDERSON

1953

M-39

PERMANENT MAGNET ALTERNATOR CONTROL BY MEANS OF MAGNETIC SATURATION

by

William L. Aitkenhead, Lieutenant, U. S. Coast Guard
B. S., U. S. Coast Guard Academy, 1946

Frank C. Anderson, Lieutenant, U. S. Coast Guard
B. S., U. S. Coast Guard Academy, 1945

Submitted in Partial Fulfillment

of the Requirements for the

Degree of Naval Engineer

from the

Massachusetts Institute of Technology

1953

PERMANENT MAGNET ALTERNATOR CONTROL BY MEANS OF MAGNETIC SATURATION

by

William L. Aitkenhead, Lieutenant, U. S. Coast Guard
Frank C. Anderson, Lieutenant, U. S. Coast Guard

Submitted to the Department of Naval Architecture and Marine Engineering on 25 May, 1953 in partial fulfillment of the requirements for the degree of Naval Engineer.

ABSTRACT

The permanent magnet alternator as a source of power has been impractical until comparatively recent times. The advent of powerful new magnetic materials similar to the "Alnico" types has made such machines more practical, and has caused renewed interest in their development and use.

One serious limitation of a permanent magnet alternator is the lack of control over the output voltage. If voltage control by means of a simple electrical means could be developed, the usefulness of the machine would be vastly increased. The purpose of the present investigation is twofold: (1) to analyze the magnetic circuit in a permanent magnet alternator when the stator becomes saturated from an independent source of magnetomotive force, and (2) to devise a means of voltage control for this type of machine.

If the stator of an alternator is visualized as a toroid and a continuous winding of many turns is wound thereon, it is possible to induce within the toroid, a continuous unidirectional flux by means of a direct current in the winding. When a permanent magnet rotor is inserted in the stator, it also tends to send flux lines through the iron of the stator. However, in portions of the stator the flux from these two separate sources tend to flow in the same direction and in portions they tend to oppose. Analysis of the magnetic circuit under these conditions shows that the air gap flux is reduced because of the overall increase in the reluctance of the flux paths facing the permanent magnet. At constant speed, the voltage is proportional to the flux in the air gap and hence if the air gap flux can be controlled the output voltage can be controlled by toroidal saturation. Furthermore the analysis and experimental verification show that the percent of voltage control by means of magnetic saturation may be increased by building into the machine additional leakage paths for the flux, although the magnitude of the voltage output is thereby reduced. The saturation of the stator appears to have no serious effects upon the waveform of a properly designed machine, or on machine heating.

PERMANENT MAGNET ELECTRICAL CONTROL BY MEANS OF MAGNETIC SATURATION

by

William L. Richmond, Lieutenant, U. S. Coast Guard
Frank C. Anderson, Lieutenant, U. S. Coast Guard

Submitted in the Department of Naval Architecture and Marine Engineering on 31 May, 1957 in partial fulfillment of the requirements for the degree of Naval Engineer.

ABSTRACT

The permanent magnet alternator as a source of power has been improved until reasonably small sizes. The advent of powerful new magnetic materials similar to the "Alnico" types has made such machines more practical, and has caused renewed interest in their development and use.

One serious limitation of a permanent magnet alternator is the lack of control over the output voltage. If voltage control by means of a simple electrical means could be developed, the usefulness of the machine would be greatly increased. The purpose of the present investigation is twofold. (1) to analyze the magnetic circuit in a permanent magnet alternator when the output voltage becomes saturated from an independent source of magnetomotive force, and (2) to devise a means of voltage control for this type of machine.

If the stator of an alternator is visualized as a toroid and a conductor winding of many turns is wound thereon, it is possible to imagine within the toroid, a rectangular differential flux by means of a direct current in the winding. Given a permanent magnet rotor is immersed in the magnetic field below to send flux lines through the wall of the stator. However, in portions of the stator the flux lines pass two separate sources tend to flow in the same direction and is getting very load to oppose. Analysis of the magnetic circuit under these conditions shows that the air gap flux is reduced because of the overall increase in the reluctance of the flux paths during the saturation regions. At normal speed, the voltage is proportional to the flux in the air gap and hence if the air gap flux can be controlled the output voltage can be controlled by magnetic saturation. Furthermore the magnetic and geometrical variables show that the control of voltage control by means of magnetic saturation may be increased by making the machine additional leakage paths for the flux, although the magnitude of the voltage output is thereby reduced. The solution of the static magnetic problem is done by graphic means using the analogy of a properly designed machine, or an electric analog.

The power expended to achieve voltage control by this method is nominal within limits, although by no means compares with the control afforded by the wound-rotor type installation. The machine tested was found to maintain constant voltage for a variable load of from 190 to 21 watts (or variation of 89%) with an expenditure of direct current power in the control winding of 23.7 watts, or 11.9% of the initial ac output power. Furthermore, the power expended for control in this device is greatest when the load power is least, making an automatic voltage regulation system using a feedback loop practical.

Two practical methods of designing more efficient control systems based on the principle of toroidal saturation are (1) develop permanent magnet materials with a higher incremental permeability (the slope of the "recovery line"), and (2) design the alternator with the maximum leakage possible consistant with the magnitude of the voltage output required.

The theoretical analysis of the magnetic circuitry is supported by the experimental results to within the accuracy of the various assumptions.

Thesis Supervisor: Professor D. C. White
Title: Assistant Professor of Electrical Engineering

ii

Cambridge, Massachusetts
May 25, 1953

Professor E. B. Millard
Secretary of the Faculty
Massachusetts Institute of Technology
Cambridge, Massachusetts

Dear Sir:

In accordance with the requirements for the Degree of Naval Engineer, we submit herewith a thesis entitled "Permanent Magnet Alternator Control by means of Magnetic Saturation".

ACKNOWLEDGMENTS

The authors wish to express their appreciation to Professor David C. White for his advice and encouragement; and to Professor Charles Kingsley, Jr. for his helpful suggestions on magnetic circuitry.

TABLE OF CONTENTS

TABLE OF CONTENTS

I. INTRODUCTION

A permanent magnet alternator is a synchronous generator which has a permanent magnet for its source of magnetomotive force instead of the wound rotor electromagnet used in the conventional alternators. As recently as 1940, permanent magnet generators were impractical because suitable magnetic materials were not available. With the advent of magnets which can better withstand the effects of temperature, demagnetizing fields, and vibration, the permanent magnet alternator is now being used in applications where a compact source of small amounts of power is required.

Permanent magnet alternators have an inherent disadvantage compared to machines excited by direct-current. Because the flux from the permanent magnet is an intrinsic quantity, there is no direct way to maintain a constant terminal voltage under varying conditions of loading and speed.

Although the characteristics of the permanent magnet cannot be altered, it is possible to regulate the output voltage of a permanent magnet alternator by establishing control over the circuit traversed by the lines of magnetic flux from the permanent magnet.

The magnetic circuit between each pair of poles of a permanent magnet rotor consists of two air gaps and a path in the iron of the stator, all in series. Control of this magnetic circuit can be obtained by either controlling the length of the air gaps or the reluctance of the path in the stator iron.

I. INTRODUCTION

A permanent magnet alternator is a synchronous generator which has a permanent magnet for its source of magnetomotive force instead of the usual rotor electromagnet used in the conventional alternator. In roughly the 1910's, permanent magnet generators were improperly because adequate magnetic materials were not available. With the advent of magnets which can better withstand the effects of demagnetization, demagnetizing fields, and vibration, the permanent magnet alternator is now being used in applications where a compact source of small amounts of power is required.

Permanent magnet alternators have an inherent disadvantage compared to conventional wound-rotor machines. Because the flux from the permanent magnets is an internal quantity, there is no direct way to maintain a constant terminal voltage under varying conditions of loading and speed.

Although the characteristics of the permanent magnet cannot be altered, it is possible to regulate the output voltage of a permanent magnet alternator by establishing control over the circuit internal to the flux of magnetic flux from the permanent magnets.

The magnetic circuit between each pair of poles of a permanent magnet rotor consists of two air gaps and a path in the iron of the rotor, all in parallel. Changing of this magnetic circuit can be effected by either controlling the length of its air-gaps or the reluctance of the path in the stator iron.

In a rotary device such as an alternator, the mechanical system necessary for adjusting the air gap length would be complex, and, in the case of a permanent magnet alternator, would nullify its chief advantage of simplicity.

The alternative method, which consists of controlling the reluctance of the stator iron, is more feasible because such control can be obtained by purely electrical means. If a coil of toroidal form were wound around the hollow cylindrical form of the stator, and a direct current were introduced in this coil, the stator iron would readily be saturated. The effect of saturating the stator iron on the reluctance of the magnetic circuit is not immediately apparent because the flux from the rotor travels in both clockwise and counter-clockwise directions in the stator between adjacent pole faces, whereas the saturation caused by the toroidal winding on the stator is due to flux traveling in but one direction in the stator.

This investigation consists of analysis and experimental verification of the results obtained by toroidal saturation of the stator iron of a permanent magnet alternator. The method of analysis and general results are applicable to all permanent magnet machines, but in order to show to what extent the output voltage can be controlled at various loads and speeds, experimental data for the particular alternator tested was used.

The alternator upon which the analysis and experimental verification were performed is shown in Fig. I. This

FIGURE 1

ALTERNATOR ASSEMBLY

alternator is a four-pole, three-phase, Y-connected machine. Its normal speed is 12,000 RPM corresponding to a frequency of 400 cycles per second. The permanent magnet rotor is of ALNICO VI. Two stators, one of USS Electrical Grade Steel, and one of HIPERNIK, were wound and tested. The stators had shallow slots milled in the outer periphery, one slot opposite each of the eighteen inner slots to admit the toroidal winding, allowing clearance for the stator to be inserted in the housing. The toroidal winding lies in the bottom of the main slots, and the generator windings are placed over the toroidal windings.

Experimental data was obtained from the machine under various conditions of saturation, loading, and speed in order to determine the effects of toroidal saturation upon the output voltage.

II. PROCEDURE

The procedure followed has been divided into two separate, but mutually supporting techniques. The first consists of an analytical solution derived from a consideration of magnetic circuit theory as applied to the peculiar magnetic circuit involved. The second procedure consists of experimental determinations of the behavior of a permanent magnet alternator when subjected to the specified conditions of magnetic saturation.

A. Analytical Procedure

The procedure used to solve the problem of the effect of saturation in the stator iron on the air-gap flux of the permanent magnet in a permanent magnet alternator is graphical in nature. The solution consists of solving two simultaneous equations in which the graphical representation of the flux versus magnetomotive characteristic of the permanent magnet provides one equation, and the flux versus mmf characteristic of the air gaps and stator iron in the magnetic circuit seen by the permanent magnet provides a second equation. The magnetizing force and flux of the permanent magnet must equal the mmf drop and the flux in the external circuit including leakage flux. For the following analysis, hysteresis is neglected so that flux versus mmf characteristics may be represented by single lines.

Determination of Rotor Characteristic

The characteristics of permanent magnets are represented by a demagnetization curve which is the second

II. PROCEDURE

The procedure followed can best be divided into two parts, but mutually supporting operations. The first consists of an analytical solution derived from a consideration of magnetic circuit theory as applied to the peculiar magnetic circuit involved. The second procedure consists of experimental determinations of the behavior of a permanent magnet alternator when subjected to the specified conditions of magnetic saturation.

A. Analytical Procedure

The procedure used to solve the problem of the effect of saturation in the stator iron on the air-gap flux of the permanent magnet in a permanent magnet alternator is graphical in nature. The solution consists of solving the simultaneous equations in which the graphical representation of the flux versus magnetomotive characteristic of the permanent magnet provides one equation, and the flux versus mmf characteristic of the air gaps and stator iron in the magnetic circuit used by the permanent magnet provides a second equation. The magnetizing force and flux of the permanent magnet must equal the mmf drop and the flux in the external circuit including leakage flux. For the following analysis, operation is confined to those flux versus mmf characteristics may be represented by single lines.

Determination of Motor Characteristic

The characteristics of permanent magnets are represented by a demagnetization curve which is the second

quadrant of the material's hysteresis loop between B_r, the retentivity, and H_c, the coercive force as shown in Fig. II. The point B_r, represents the flux density of the magnet when it is magnetically short-circuited; when the magnet is subjected to a demagnetizing force such as an air-gap line Oa, the point representing the operating condition moves along the demagnetization curve from B_r to point a, and B_a is the flux density in the air gap. If the air gap is increased in length until the air-gap line becomes Ob, the operating point will move down the demagnetization curve from a to b, and the resulting flux density will then be B_b. If the gap is decreased, the operating point will not return along the demagnetization curve, but will travel along a minor hysteresis loop such as bd. For example, if the air-gap line is again Oa, the operating point will become point d, and the flux density becomes B_d. [1]

In order to determine the characteristics of the permanent magnet rotor, it is necessary to determine the slope of the minor hysteresis loop, otherwise known as the "recovery line", and the position on the demagnetization curve where the recovery line originates. The origin of the recovery line does not necessarily represent the point on the demagnetization curve where the magnetic open-circuit air-gap line intersects the demagnetization curve because the magnet may have been subjected to a demagnetization force in excess of the open-circuit air-gap condition. This would put the open-circuit operating point on the

FIGURE II

PERMANENT MAGNET BEHAVIOR

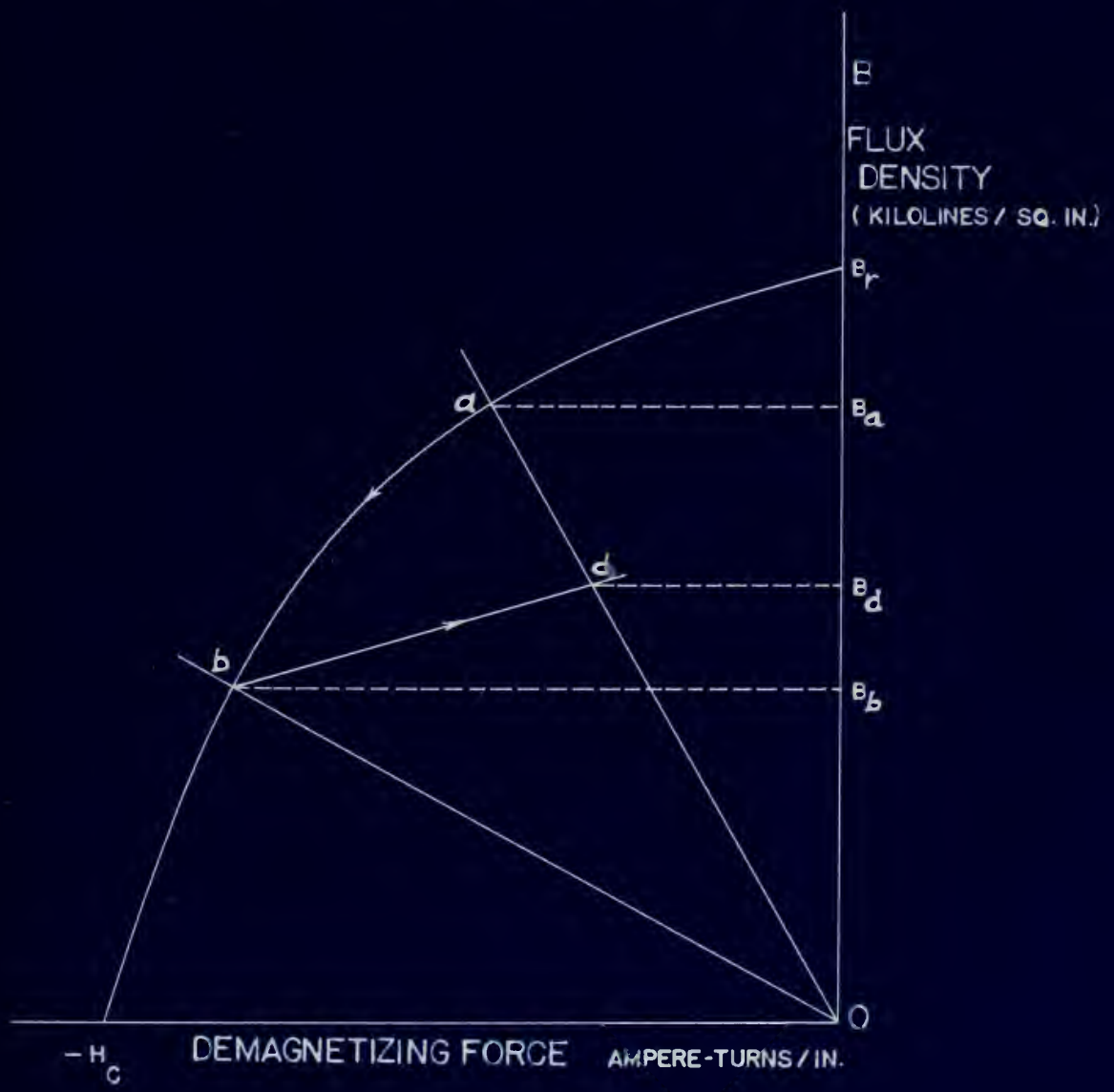

intersection of the open-circuit air-gap line and a recovery line whose origin is closer to H_c on the demagnetization curve (Fig. II). A point on the recovery line of the permanent magnet rotor can be determined by measuring the open-circuit flux per pole with a fluxmeter and plotting this value of flux on the open-circuit air-gap line.

Methods have been devised [2] to determine the open-circuit air-gap line for magnets which do not have a well defined air gap. Scott [3] found that a definite relation exists between the ratio of length-to-diameter of round bar magnets and the flux in the air between poles. This relationship is expressed by a curve of B/H versus l/d (Fig. III) where B/H is the slope of the open-circuit air-gap line, also called the "permeance coefficient", and l/d is the length-to-diameter ratio of the bar magnet. The relationship holds within a fair degree of accuracy to magnets other than round bar magnets provided that, if the magnet is curved, the poles are not too close together. To apply Scott's bar magnet theory to the multipolar shape of a permanent magnet rotor, an equivalent bar magnet is assumed by estimating the length of the mean flux path between adjacent pole faces to provide the dimension, l (Fig. IV); an equivalent diameter is established by assuming the pole face of the magnet has the diameter of a circle of the same area as the pole face [3] :

$$d = \sqrt{\frac{4A}{\pi}} \qquad (1)$$

$$q = \sqrt{\frac{\mu}{\rho c}} \qquad (1)$$

a circle of the same area as the pole face [8] .

measuring the pole face of the magnet (as the diameter of 1 (Fig. IA)) an equivalent diameter is calculated by

between adjacent pole faces to provide the "inscribed"

measured by estimating the length of the mean flux path

of a permanent magnet rotor," an equivalent air magnet is

To apply Sonte's bar magnet theory to the multipolar shape

magnets other than round bar magnets physical size. If the

relationship holds within a fair degree of accuracy to

is the length-to-diameter ratio of the bar magnet. The

gap line" also called the "permeance coefficient", and l/d

(Fig. III) where B/H is the slope of the open-circuit air-

relationship is expressed by a ratio of B/H versus l/d

bar magnets and the flux in the air gap(s) yield. This

ratios between the ratio of length-to-diameter of round

defined air gap. Sonte [3] found that a definite relation

circuit air-gap line for magnets which do not have a well

Methods have been derived [1] to determine the open-

end line.

mag plotted this value of flux on the open-circuit air-

measuring the open-circuit flux per pole with a flux meter

line of the permanent magnet motor can be determined by

demagnetization curve (Fig. 12). A point on the recoil

FIGURE III

PERMEANCE COEFFICIENTS OF EQUIVALENT BAR MAGNETS

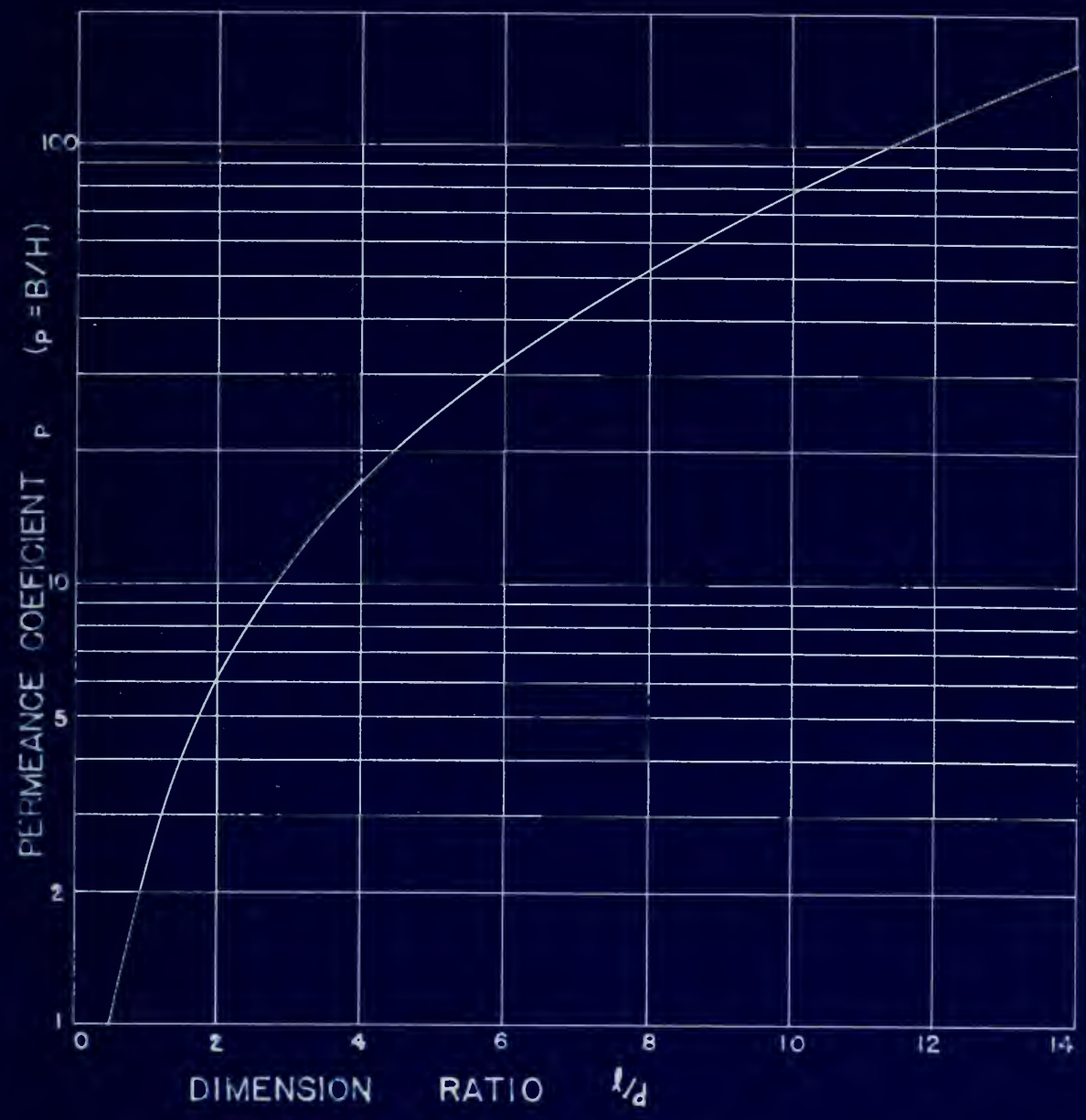

FIGURE IV

FLUX PATHS IN ROTOR

Having assumed an equivalent l/d, enter the curve of Fig. III and determine the slope of the open-circuit air-gap line, B/H. This value of B/H in conjunction with the measured flux of the magnet establishes the open-circuit operating point of the permanent magnet.

The slope of the recovery line, called the "incremental permeability", can be obtained from manufacturer's literature [4], where the slope of the recovery line is given in the form of a graph of incremental permeability versus the flux density at point of reversal for various magnetic materials. Knowing that the recovery line must pass through the operating point on the open-circuit air-gap line, the slope of the recovery line is determined.

An estimate of the flux versus mmf characteristic for the permanent magnet rotor has now been established. When the rotor is inserted in the stator, the operating point of the magnet will lie on this recovery line. Fig. V shows this flux versus mmf characteristic.

Determination of Stator Characteristic

To visualize the approach used to determine the stator characteristic, consider the rotor inserted in the stator. The lines of flux from a magnet pole will cross the air gap and split into two parallel paths in the stator iron and close on themselves through adjacent pole faces. Leakage flux from the permanent magnet will also exist, but this flux does not appear in the stator magnetic circuit and can be considered separately.

FIGURE V

DETERMINATION OF RECOVERY LINE

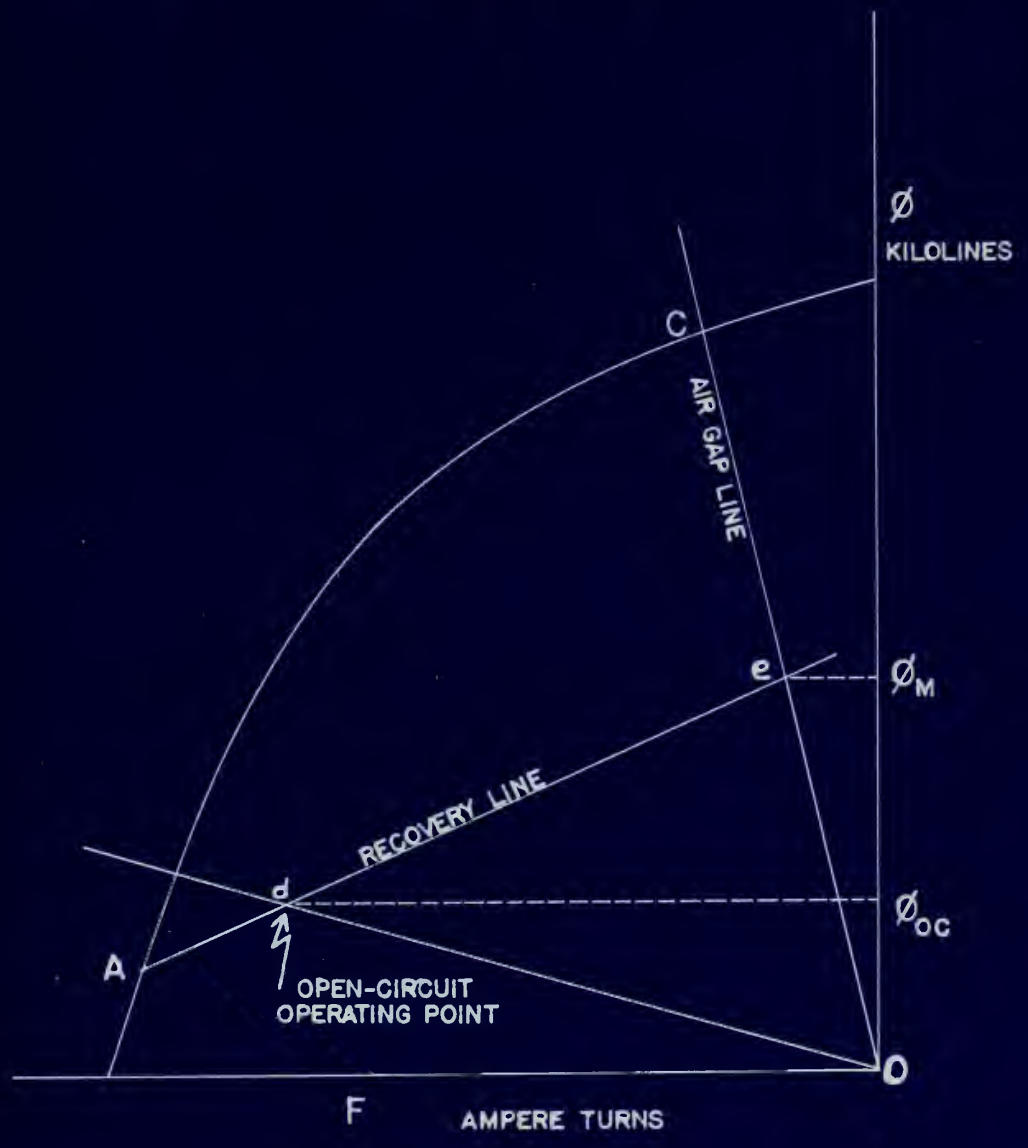

Using an electric circuit analogy in which reluctance is analogous to resistance, flux to current, and magnetomotive force to voltage, the magnetic circuit is represented in Fig. VI. The effect of $R_{(air\ gap)}$ can be represented by an air-gap line in the stator characteristic. The effect of R_1 and R_2, the reluctances of the stator iron paths which are to be saturated by the toroidal winding, can be analyzed separately and added graphically to the air-gap line to obtain the overall magnetic characteristic of the magnetic circuit external to the rotor. Temporarily neglecting the air gap and leakage paths, we now have the analogous circuit shown in Fig. VII. It is to be emphasized that electric circuit analogies are for illustrative purposes only, and that the equations resulting therefrom must always require a graphical solution because of the non-linear nature of reluctance.

Now consider the stator, without the permanent magnet rotor, as a toroid with a continuous winding around it as shown by Fig. VIII. A direct current in the toroidal winding will cause a magnetomotive force between points a and b

$$F_c = F_{ab} = \phi_1 R_{ab} \qquad (2)$$

where R is the reluctance and F_c is the ampere turns in half the toroid. The electric circuit analogy may be represented by Fig. IX.

If the circuit of Fig. IX were cut in half at line

FIGURE VI

ELECTRIC CIRCUIT ANALOGY

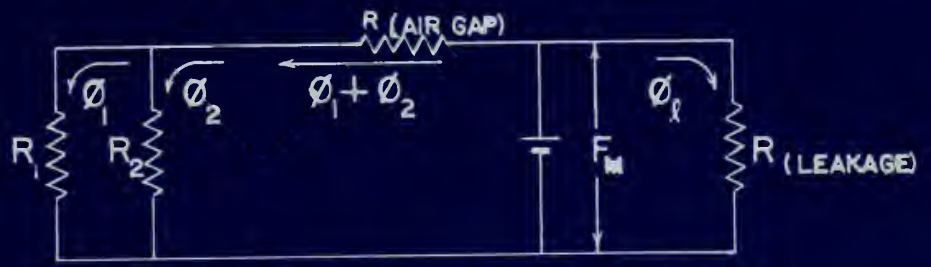

NOTE: R_1 AND R_2 REPRESENT THE RELUCTANCE IN EACH PATH OF THE STATOR IRON

FIGURE VII

ELECTRIC CIRCUIT ANALOGY OF STATOR

AIR GAP AND LEAKAGE NEGLECTED

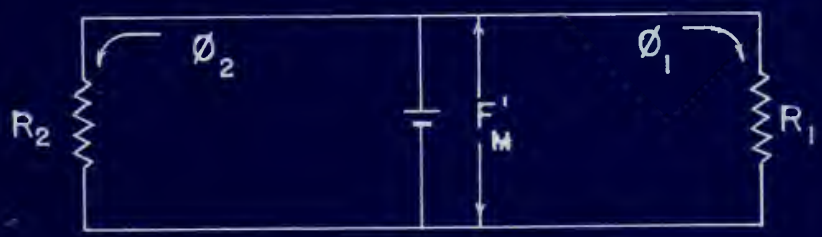

FIGURE VIII

TOROIDAL WINDING

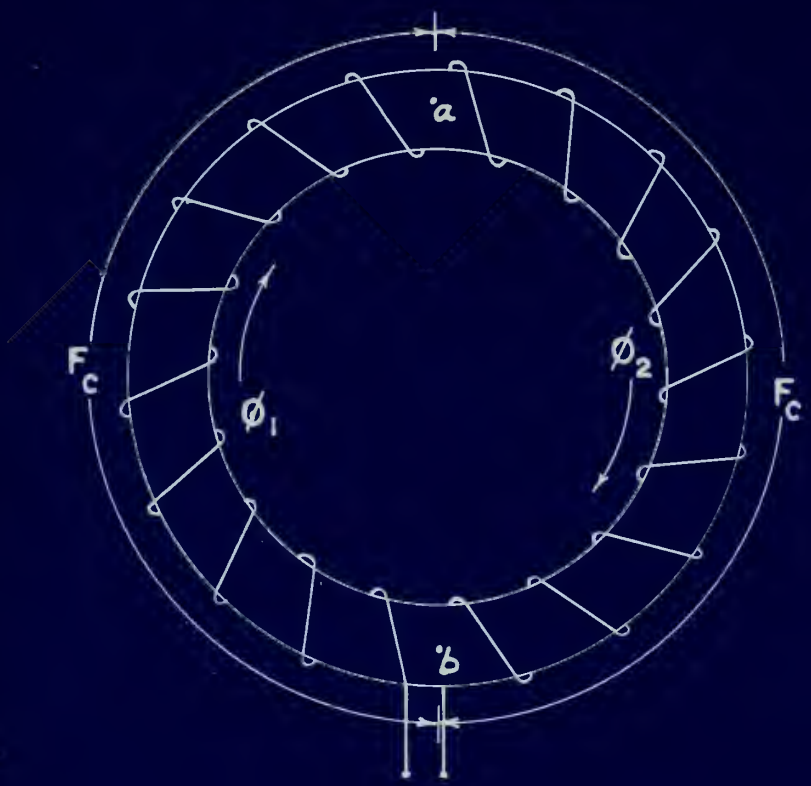

FIGURE IX

ELECTRIC CIRCUIT ANALOGY OF TORCID ONLY

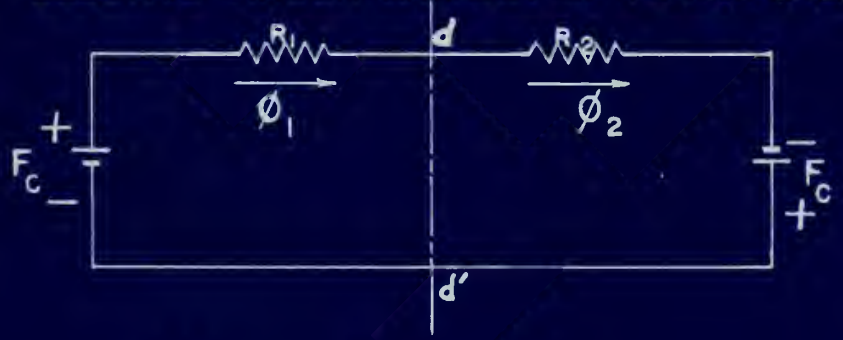

NOTE: $F_C = \phi R$

d-d' by a magnetic short-circuit, the flux in each side would be unchanged:

Half of circuit shorted:

$$(1)\quad F_c = \phi_1 R \;;\; \phi_1 = F_c/R \;;\text{ shown in Fig. X} \qquad (3)$$

Both halves of circuit in series:

$$(2)\quad 2F_c = \phi_1(2R) \;;\; \phi_1 = F_c/R \text{ as before.} \qquad (4)$$

The above case is not to be confused with the case of the curve of ϕ versus H, where doubling H (amperes turns per inch) would give, in effect, 2F acting to produce ϕ.

Having established the circuit behavior with no magnet inserted, we can now proceed to find the effect of adding the permanent magnet rotor. For simplicity of illustration, a two-pole magnet is used, but the same conclusions will be valid for multipolar rotors. The effects of the air gap and leakage are still temporarily neglected.

The resulting electric circuit analogy is illustrated by Fig. XI.

The following equations apply:

In left half of the circuit A:

$$(F_c - F_m') = R_a(\phi_1 - \phi_{m1}') = R_a\,\phi_A \qquad (5)$$

In right half of the circuit B:

$$(F_c + F_m') = R_b(\phi_1 + \phi_{m2}') = R_b\,\phi_B \qquad (6)$$

and

$$\phi_m' = (\phi_{m1}' + \phi_{m2}')$$

d-d' by a magnetic short-circuit, the flux in each side would be unchanged:

Half of circuit shorted:

$$(1)\quad \mathcal{P}^c = \mathcal{P}^T_R \;;\; \mathcal{P}^T = \mathcal{P}^c_R \text{ ; shown in Fig. 7} \qquad (7)$$

Both halves of circuit in series:

$$(2)\quad \mathcal{P}^c = \mathcal{P}^T(2R) \;;\; \mathcal{P}^T = \mathcal{P}^c_R \text{ as before.} \qquad (8)$$

The above case is not to be confused with the case of the curve of $\mathcal{P}$ versus R, where doubling R (keeping turns per inch) would give, in effect, 2P acting to produce $\mathcal{P}$.

Having established the circuit behavior with no magnet inserted, we can now proceed to find the effect of adding the permanent magnet rotor. For simplicity of illustration, a two-pole magnet is used, but the same conclusions will be valid for multipolar rotors. The effects of the air gap and leakage are still temporarily neglected.

The resulting electric circuit analogy is illustrated by Fig. XI.

The following equations apply:

In left half of the circuit A:

$$(\mathcal{P}^c - \mathcal{P}^m_R) = \mathcal{R}^m(\mathcal{P}^T - \mathcal{P}^{mT}_R) = \mathcal{R}^m\,\mathcal{P}^m \qquad (9)$$

In right half of the circuit B:

$$(\mathcal{P}^c + \mathcal{P}^m_R) = \mathcal{R}^m(\mathcal{P}^T + \mathcal{P}^{mT}_R) = \mathcal{R}^m\,\mathcal{P}^m \qquad (6)$$

and $\mathcal{P}^m_R = (\mathcal{P}^{mT}_R + \mathcal{P}^{mT}_R)$

FIGURE X

DC MAGNETIZATION CURVE —
IN TERMS OF FLUX AND MAGNETOMOTIVE FORCE

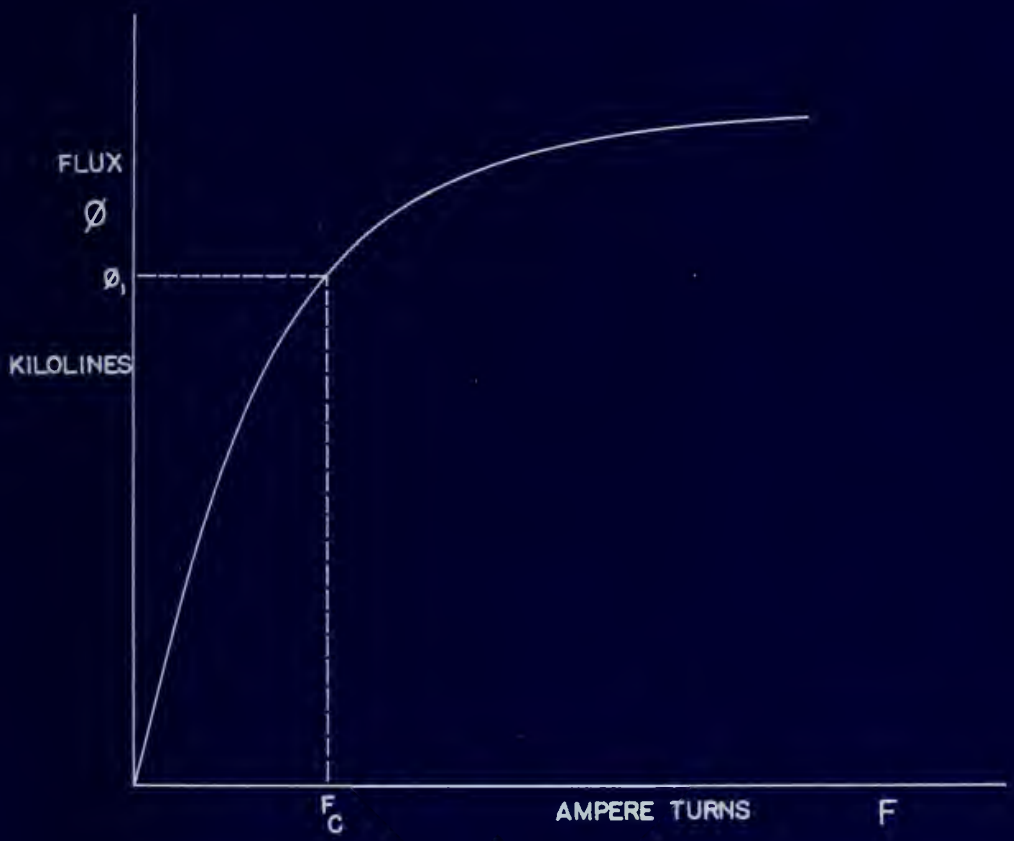

It is also obvious that $\phi_B - \phi_A = \phi_m'$ (7)

since $(\phi_1 + \phi_{m1}') - (\phi_1 - \phi_{m2}') = \phi_m' =$ Flux through the permanent magnet (neglecting leakage effects) (8)

For the actual solution the graphical representation of reluctance (i.e.: the magnetization curve) must be used as shown in Fig. XII.

It now becomes desirable to develop a simple graphical method of expressing ϕ_m' versus F_m'. In Fig. XIII, consider the point P on the demagnitization curve at F_c to be the "operating point". Then for each value of F_m' (the mmf imposed between points ab by the permanent magnet) (see Fig. VIII), add the ordinates $[(\phi_1 + \phi_{m2}') - \phi_1]$ and $[\phi_1 - (\phi_1 - \phi_{m1}')]$ to give the ordinate ϕ_m'. If a new curve is now plotted with the origin taken at P, the result will give a curve of ϕ_m' versus F_m' as shown in Fig. XIV.

Figure XIV may now be reversed and plotted directly on the demagnitization quadrant of the rotor, sheared* into the air gap line†, and corrected for leakage‡. The correction for air gap and leakage will yield a curve of F versus ϕ_m, the same coordinate system as the recovery line. Therefore the point of intersection of these two curves represents the flux through the permanent magnet

---

* See "Details of Shearing" Appendix A
† See "Calculation of Air Gap Line" Appendix A
‡ See "Estimate of Flux Leakage" Appendix A

curves represents the flux entering the permanent magnet
line. Therefore the point of intersection of these two
F values h_m^{pm}, the same coordinate system as the load line
connection for air gap and leakage will yield a curve of
the air-gap line[†] and considered the leakage[‡]. The
demagnetizing waveform of the motor, obtained* into
Figure 31A may now be reversed and plotted directly on
give a curve of h_m^{pm} versus λ_m^{pm} as shown in Fig. 31B.
is now plotted with the origin taken at F_1, the result will
$\left[F^1 - (h^1 - h_{sl}^{pm})\right]$ to give the relation h_m^{pm}. If a new curve
Fig. VIII), add the variance $\left[(h^1 + h_{sl}^{pm}) - h^1\right]$ and
imposed between points ab by the permanent magnet) (see
"operating point". Then for each value of λ_m^{pm} (the net
the point P on the demagnetization curve at λ_1 to be the
method of expressing h_m^{pm} versus λ_m^{pm}. In Fig. XIII, consider

It now becomes desirable to develop a simple graphical
as shown in Fig. XII.

For the normal solution the graphical interconnection
of reluctance (i.e.: the magnetization curve) must be used
(neglecting leakage effects)
through the permanent magnet

since $(h^1 + h_{sl}^{pm}) - (h^1 - h_{sl}^{pm}) = h_m^{pm}$ Flux (6)

It is also obvious that $h_m^{pm} - h_g^{pm} = h_{sl}^{pm}$ (7)

---

* See "Details of Procedure" Appendix B
† See "Calculation of Air Gap Line" Appendix A
‡ See "Derivate of Flux Leakage" Appendix A

FIGURE XI

ELECTRIC CIRCUIT ANALOGY WITH ROTOR IN PLACE

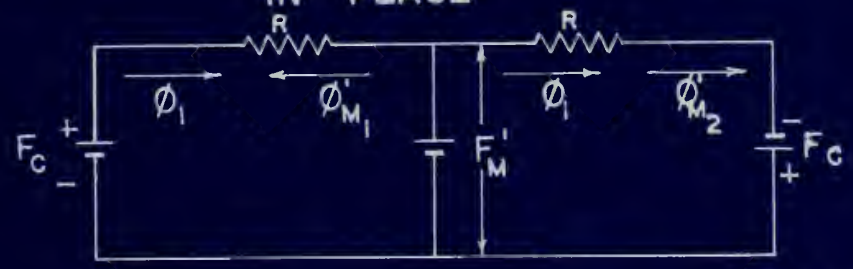

NOTE: F'_M IS THE MMF IMPOSED BETWEEN THE POINTS $a-b$ OF THE STATOR

FIGURE XII

GRAPHICAL SOLUTION FOR ϕ'_M

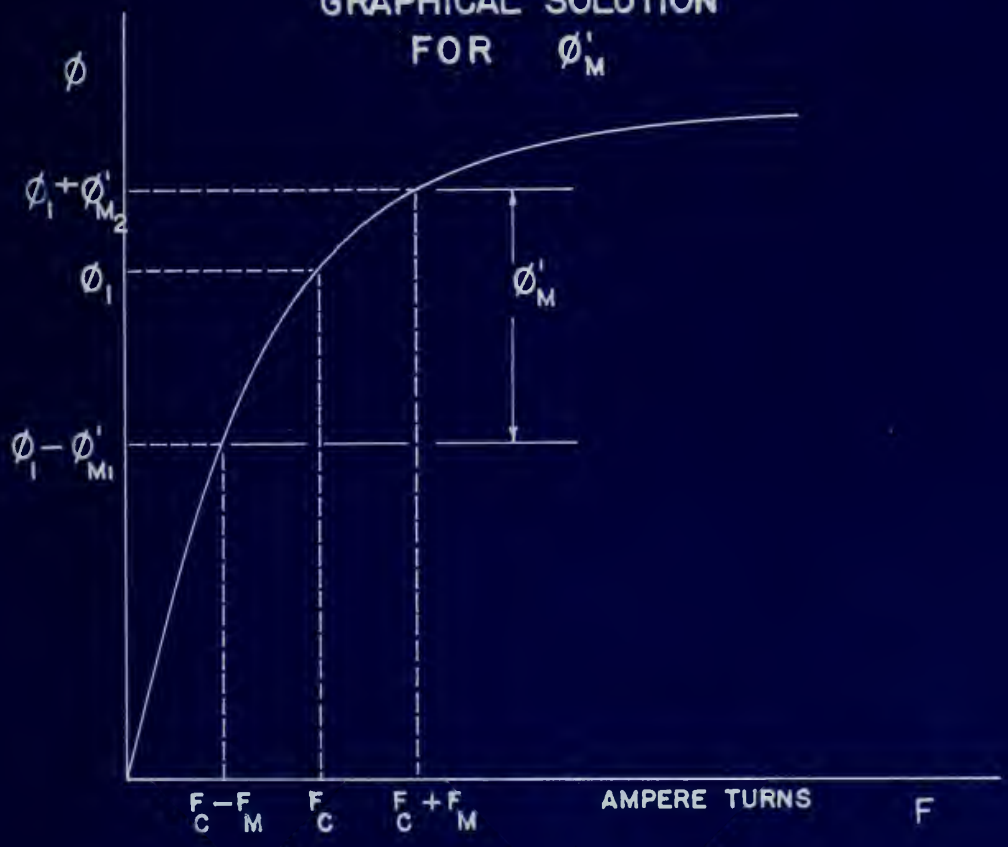

FIGURE XIII

GRAPHICAL SOLUTION

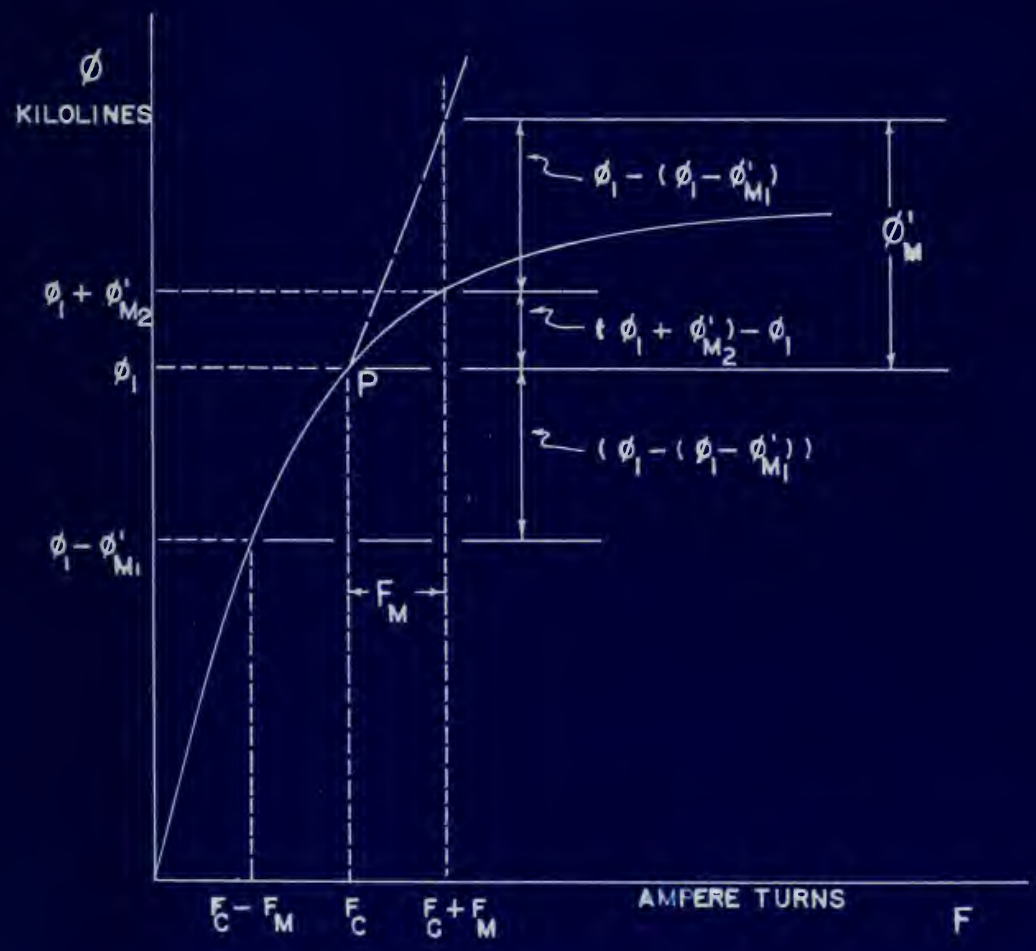

FIGURE XIV

ϕ'_M VS. F_M CURVE

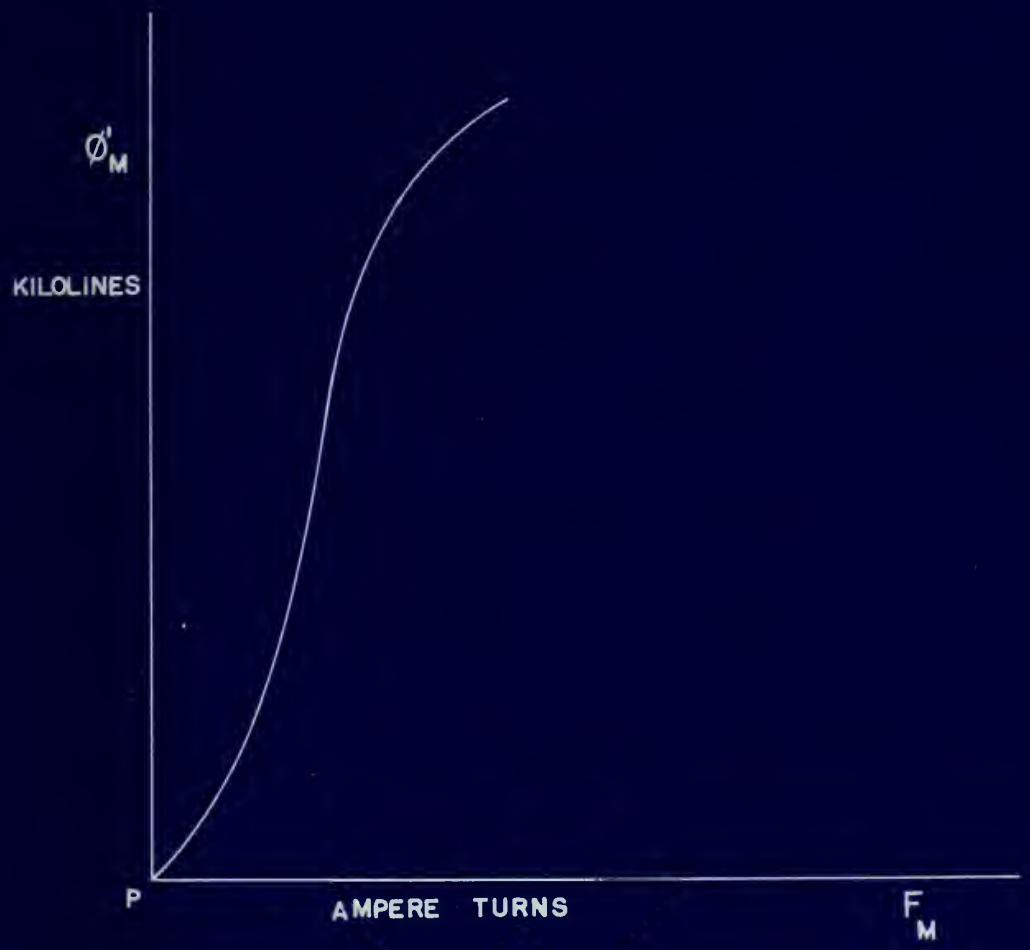

under existing conditions. Because of the nearly vertical slope of the ϕ_m' curve, the leakage correction is small and negligible error is introduced, percentage wise, by neglecting it. Therefore the ϕ_m' versus F_m curve may be used for the solution of the simultaneous (graphical) equations of the magnetic circuit.

The leakage is estimated as a function of magnetic potential drop in the circuit, and is assumed to be linear*. It is shown as line OL on Fig. XV. The effect of this leakage is to reduce the useful flux, and therefore at any value of F or U (magnetic potential drop in ampere turns), the leakage flux must be subtracted from the magnet flux, to give the useful flux. This can be shown as having the same effect as a change in the slope of the recovery line of the magnet would have, and the results may be shown as a "virtual recovery line" on Fig. XV. The intersection of the reversed ϕ_m versus F_m curve with the "virtual recovery line" will now provide a solution for the state of useful flux in the air gap.

Furthermore it is readily seen that as the direct current in the toroidal winding is varied, (F_c is varied), the shape of the ϕ_m versus F_m curve changes as shown in Fig. XVI.

Hence when these curves are reversed and plotted on the demagnitization curve as before, and corrected for the air

---

* See "Estimate of Flux Leakage" Appendix A

FIGURE XV

CIRCUIT CHARACTERISTICS PLOTTED ON MAGNET CHARACTERISTICS

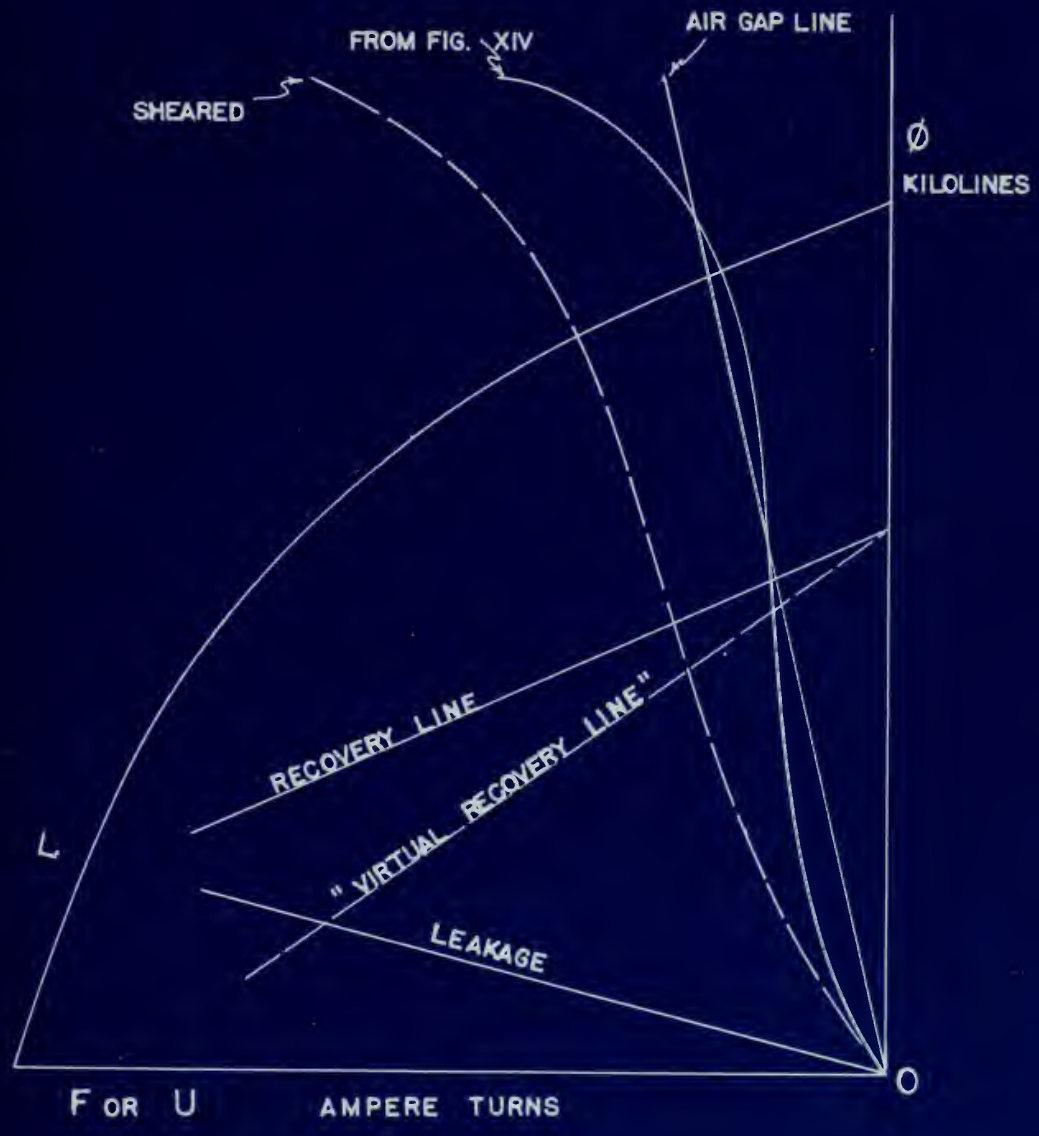

FIGURE XVI

EFFECT OF F_C ON THE ϕ'_M VS. F_M CURVE

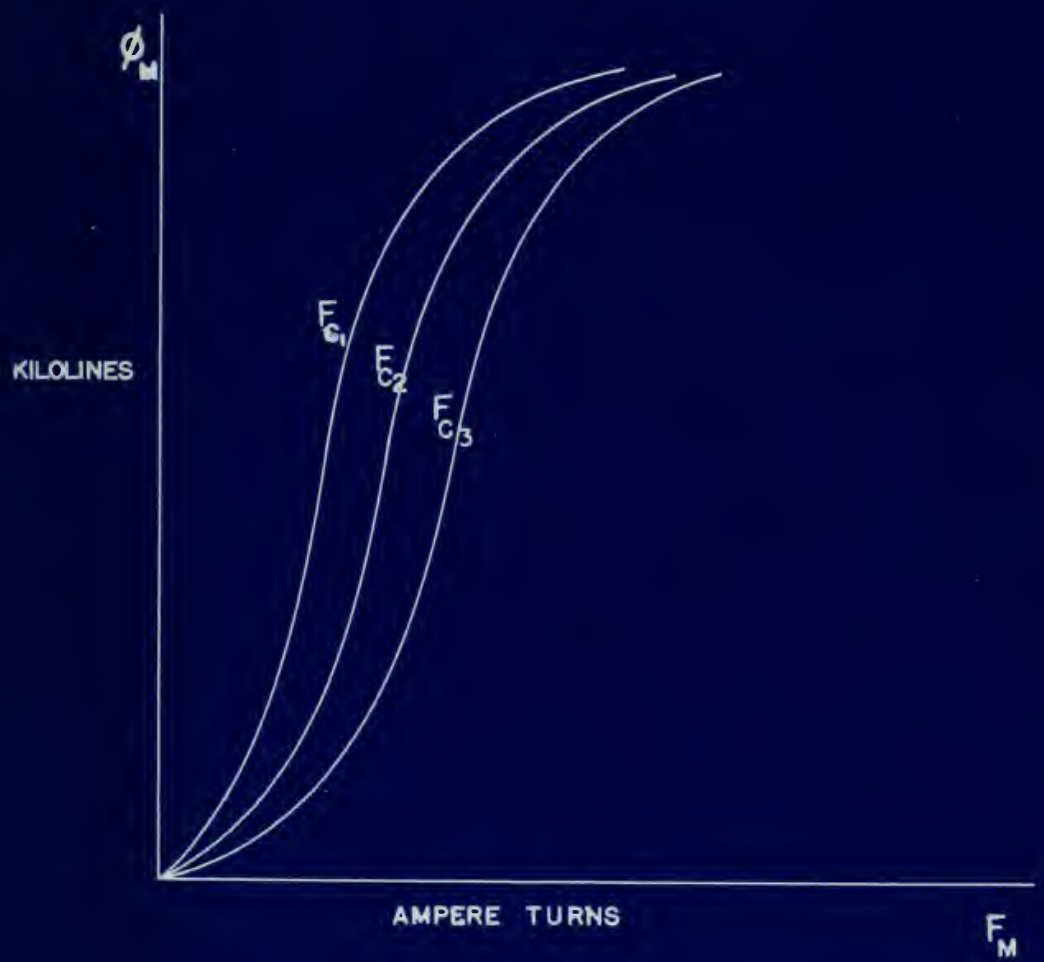

gap, the intersection with the "virtual recovery line" moves progressively toward the left, as shown in Fig. XVII, and the effective air gap flux ϕ_g is thereby decreased.

If the alternator is running at constant speed, a common occurrence in synchronous machines, the voltage output will be directly proportional to the useful gap flux ϕ_g, and we have therefore established a method of control over the output voltage of a permanent magnet alternator.

B. Experimental Procedure

In order to verify the effectiveness of controlling a permanent magnet alternator by saturation of the stator iron, two stators, one of USS Electrical Grade Steel, and one of HIPERNIK were wound with coils of toroidal form, in addition to the normal three-phase winding. Tests of performance were made under varying conditions of saturation, loading and speed. The data obtained was correlated in a series of graphs illustrating the characteristics of this type of voltage control.

The load circuit used for testing the permanent magnet alternator consisted of a three-phase, y-connected, balanced load.

A Ward-Leonard system prime mover driving the alternator through a 1.5:10 V-belt drive was found to be the most effective means for maintaining constant alternator speeds. No synchronous drive of usable size was available; moreover, a synchronous drive would limit the test frequency to but one value.

be put one value.

Moreover, a synchronous drive would limit the user impedance
to 0 ohms or nearly zero. No synchronous drive of nearly size was available!
effective means for maintaining constant alternator speeds,
through a 1,310 I-watt drive was found to be the most
A Ward-Leonard system drive motor driving the alternator
load.

The load circuit used for testing the parameter meters
characteristics of this type of voltage control.
correlated in a series of graphs illustrating the
operation, loading and speed. The data obtained was
performance were made under varying conditions of
addition to the normal three-phase winding. Taps of
use of NINETEEN were wound with coils of counter form, in
line, two starting, one of TEN Electrical Degree Travel, and
a permanent magnet alternator by saturation of the static

B. Experimental Procedure

In order to verify the effectiveness of controlling
over the output voltage of a permanent magnet alternator.
R_B, and we have therefore established a method of control
output will be directly proportional to the neutral gap flux
common connection is synchronous machines, the voltage
If the alternator is running at constant speed, a
and the effective air gap flux ϕ_g is thereby decreased.
move progressively toward the left, as shown in Fig. XVII.
gap, the intersection with the "virtual reactive line"

FIGURE XVII

EFFECT OF F_c ON AIR GAP FLUX

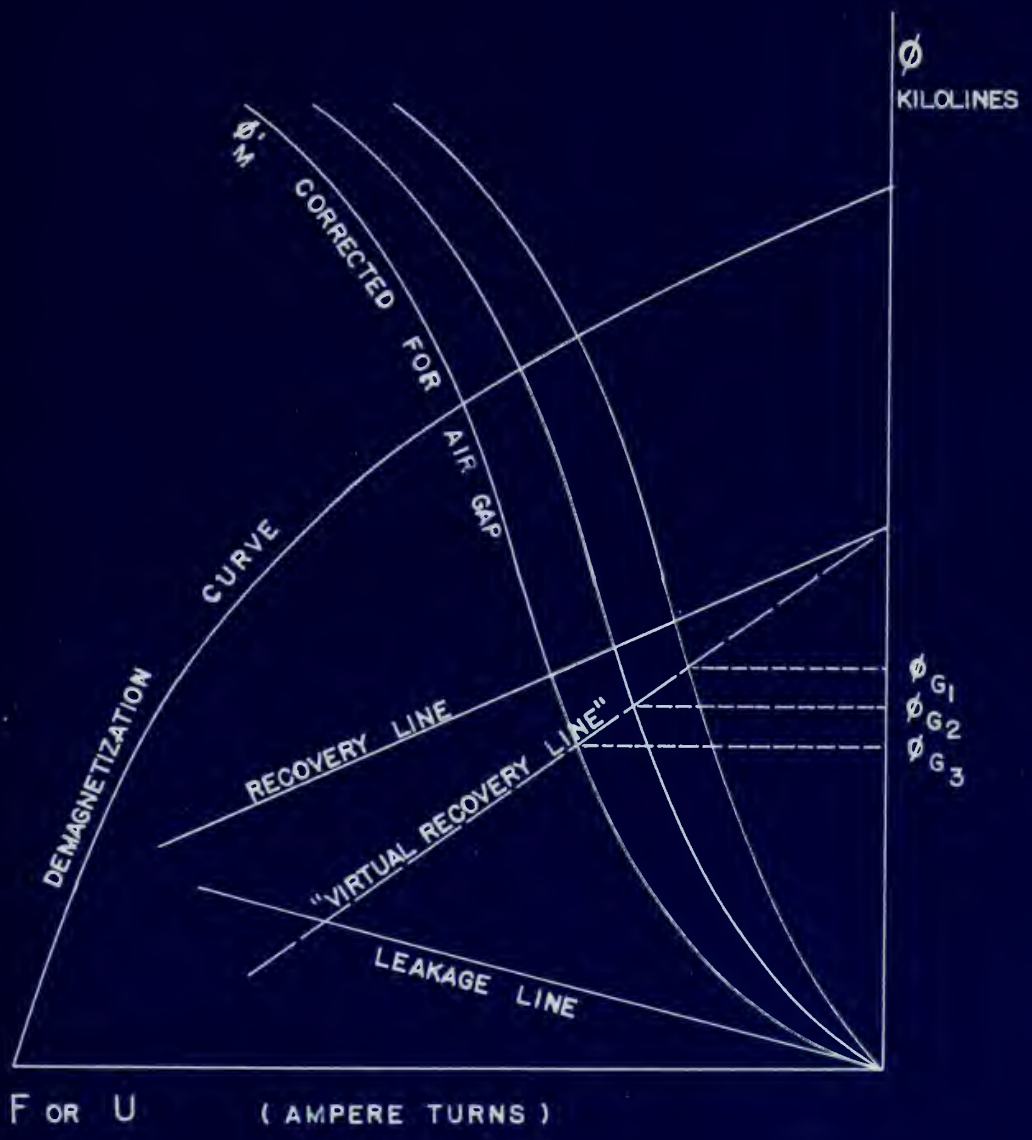

The frequency for each test was set by maintaining a Lissajou pattern on an oscilloscope, an oscillator being used to measure the frequency.

The load resistance were slide-wire rheostats which were balanced at various values of resistance with a calibrated ohmmeter. In the tests where an inductive load was used, standard 100 millihenry inductances were connected in series with slide-wire rheostats so that the resistive part of the load could be balanced also.

Data was taken at given constant frequencies and load resistances. Control current was varied from 0 to 8 amperes in one ampere steps; at each value of control current, the generator load current and terminal voltage were read on rms-reading thermocouple instruments. The data recorded was direct-current control current, alternating-current terminal voltage, and alternating-current load current.

From the load current measured, the alternating-current real power was computed by the equation:

$$P = 3I^2R_L \qquad (9)$$

Otherwise, the data taken was used directly in plotting the curves showing the results.

The results obtained from tests on the USS Electrical Grade stator are of limited value because it was found that the toroidal control winding developed multiple grounds when the stator was inserted in the stator housing. Because

of these grounds, the ampere-turns of control mmf could not be established and no control current-terminal voltage relationship could be established. Nevertheless, current in the control winding had a definite effect on the generator terminal voltage.

Usable results were obtained from the HIPERNIK stator.

A summary of the test conditions for the tests on the HIPERNIK stator are as follows:

Frequency (cycles per second)	400	350	300
Load Resistance (ohms per phase)	open circuit 46.5 93.0 139.5	open circuit 46.5 93.0 139.5	open circuit 46.5 93.0 139.5
Inductive Load (per phase)	100 mh + 100 ohms	100 mh + 100 ohms	100 mh + 100 ohms

Tests on the HIPERNIK stator with an auxiliary flux leakage path were made. The auxiliary leakage path consisted of HIPERNIK discs clamped to each end of the rotor, but separated from the rotor by non-magnetic TEFLON spacers:

No. of 0.01" TEFLON spacers	2	2	2
No. of 0.014" HIPERNIK discs	1	2	2
Frequency in cps	400	400	350
Load in ohms/phase	open circuit 100	open circuit 100	open circuit 100

III. RESULTS

Experiment and analysis establish the following results:

1. The generator terminal voltage can be reduced, by means of the control winding, to a smaller value than the terminal voltage before control current is applied to the control winding. This reduction is caused in part by an actual reduction in flux from the magnet, and in part by an increase in the portion of magnet flux that traverses the leakage paths.

2. The percent of voltage control is directly dependent on the flux leakage path seen by the permanent magnet rotor.

3. The percent voltage reduction of item (1) is independent of the generator load current and power factor of the current, although the magnitude of voltage reduction is proportional to the initial voltage.

4. The relation between control current and terminal voltage is linear, provided the leakage paths do not saturate:

$$E = E_1 - KI_{dc} \quad \text{or} \quad \phi = \phi_1 - KI_{dc} \tag{10}$$

5. The wave shape of the terminal voltage is not affected, except in amplitude, by the saturation of the stator iron by the control current, provided the stator is designed so that harmonics are negligible. In the USS Electrical stator, which was designed with a slot skew, no harmonics were noticeable on the oscilloscope and the wave shape was not noticeably affected by saturation. In the

Adjustment and operating sequence for fully-automatic operation

2. The generator terminal voltage can be reduced, by means of the control rheostat, to a smaller value than the terminal voltage before control current is applied to the control winding. This reduction is caused in part by the actual reduction in flux from the magnet, and in part by an increase in the portion of magnet flux that traverses the locking path.

3. The amount of voltage control is directly dependent on the flux locking path used by the permanent magnet rotor.

3. The percent voltage reduction at item (1) is independent of the generator load current and power factor of the current, although the magnitude of voltage reduction is proportional to the initial voltage.

4. The relation between control current and terminal voltage is linear, provided the locking path is not saturated.

$$E = E_1' - KI_{CO} \quad \text{or} \quad E = E_1' - KI_{CO} \tag{10}$$

5. The wave shape of the terminal voltage is not affected, except in amount, by the application of the shunt line by the control rheostat, provided the rotor is designed so that harmonics are negligible. In the GE Universal Rotor, which was designed with a slot skew, no harmonics were contained in the oscillograms and the wave shape was not noticeably affected by saturation. In the

HIPERNIK stator which, for reasons of economy, was constructed with straight slots, some effects on harmonics due to stator saturation were noticed.

6. The magnetic material of the stator has negligible effect on voltage control providing the material is magnetically soft and is unsaturated when no control current is applied.

7. There is no net voltage induced in the toroidal winding by the air gap flux.

IV. DISCUSSION OF RESULTS

The two stators were wound and tested in order to determine the effect of different magnetic materials on the regulation of the generator output voltage when controlled by a direct-current toroidal winding. The four-pole Alnico VI permanent magnet rotor, the cast aluminum stator housing, and the two stators are illustrated in Fig. I. The detailed drawings of the stator and rotor appear in Fig. XX.

The generator prime mover consisted of a direct current motor, supplied from a direct current motor-generator set with field control. Frequency of alternator voltage was continuously checked by means of an oscilloscope.

Tests were performed under balanced resistive loads from no load to heavy loads, and one test was performed under a lagging reactive load of 0.37 power factor. Tests were conducted at 400, 350, and 300 cycles per second.

The first stator tested was of USS Electrical Grade Steel with a direct-current toroidal control winding of 162 turns of 24 gauge wire. This stator had a slot skew of one slot pitch. However this stator was found to have multiple grounds in the toroidal winding, and therefore the data must be considered of limited value. The second stator was of HIPERNIK with a toroidal winding of 198 turns of 24 gauge wire. Appendix A gives the details of the generating windings, and the magnetic properties of USS Electrical Grade Steel and HIPERNIK are given in Appendix B.

For the particular HIPERNIK stator tested, it was found

that the generator terminal voltage for a given load could be reduced to 63 per cent of its initial value by applying direct current to the toroidal control winding. Further control could have been obtained by applying larger amounts of control current at the expense of increased I^2R losses in the control winding. The final limitation on the amount of control is that the permanent magnet rotor should not be subjected to a knockdown lower than the existing knockdown point on its demagnetization curve.

Considering the expression for generated voltage:

$$E = K \phi n \tag{11}$$

and assuming the terminal voltage of the generator at a given load is to be held constant, then:

$$\phi n = K' \tag{12}$$

and the relation between ϕ and n must be a hyperbola. The speed of the generator can vary along the hyperbola within certain limits, determined by the amount ϕ can be changed by the control winding, and yet maintain a constant terminal voltage.

The relation between the control current I_c and the effective air gap flux ϕ is nearly a straight line with negative slope. (See Fig. XXVIII). Within a limited range, the flux may be considered to vary inversely with a control current.

$$\phi = \frac{K}{I_c} \tag{13}$$

$$k = \frac{1}{\sigma^2} \tag{12}$$

Therefore at constant terminal voltage,

$$\phi n = K'' \tag{14}$$

$$\frac{n}{I_c} = K'' \tag{15}$$

$$\text{or} \quad n = K''' I_c \tag{16}$$

and the relation between speed (or frequency) and control current may be seen to be a straight line. This is borne out by the experimental results. (See Fig. XXXVIII).

Since ϕ decreases linearly with control current, and the power dissipated in the control winding increases as the square of the control current, it is seen that the range of voltage control obtained is limited by increased power consumption in the control winding.

The linear relation between control current and terminal voltage can be explained by consideration of the graphical solution of the problem. It is found that control current moves the characteristic of the stator, (ϕ_m' in Figure XIV), an equal amount to the right for each unit increase in control current. Since the point of intersection of the ϕ_m' curve and the permanent magnet recovery line occurs in the linear region of the ϕ_m' curve, the point of intersection follows a linear relation.

Analytically it can be seen by expressing the linear portion of the ϕ_m' curve as:

$$\phi_m' = aF - b\, I_{dc} \tag{17}$$

The "virtual" permanent magnet recovery line may be expressed as:

$$\phi_{gap} = C - dF \qquad (18)$$

Figure XVIII shows these expressions in graphical form plotted on conventional coordinates.

Solving for ϕ_g:

$$\phi_g = A - B\, I_{dc} \quad \text{or} \quad \phi_g = \phi_1 - k\, I_{dc} \qquad (19)$$

For any initial value of ϕ_1 for a given load, the above expression for ϕ_g holds, thus the per cent reduction of the initial voltage is independent of the load current drawn.

If the generator were driven by a constant speed drive, it is possible to maintain a constant terminal voltage from no load to full load by means of the control winding. Moreover, if the power for the control winding were to be obtained from the generated output, the control power would be least when the power demand on the generator were the greatest. (See Fig. XXXVI). That the amounts of control power required for certain applications is practical is indicated by Figs. XXXVI and XXXVII, in which the control winding is used to maintain constant terminal voltage for (1) variable power consumption by the load, and (2) variable generator speed from 9,000 RPM to 12,000 RPM.

The control of terminal voltage under all load conditions, and with variations in prime mover speed appears

The "virtual" incremental plastic resistivity line may be
expressed as:

$$R^{p}_{inc} = 0 - \alpha_R \qquad (29)$$

Figure XVIII shows these expressions in graphical form
plotted on coordinates coordinates.

Solving for R^{p}_{B}:

$$R^{p}_{B} = A - B\,T_{Ba} \quad \text{or} \quad R^{p}_{B} = R^{e}_{B} - R\,T_{Ba} \qquad (30)$$

The only initial value of R^{p}_{B} for a given load, the
above expression for R^{p}_{B} holds, since the per cent reduction
of the initial voltage is independent of the load current
drawn.

If the generator were driven by a constant speed motor,
it is possible to maintain a constant terminal voltage from
no load to full load by means of the control winding.
However, if the power for the control winding were to be
obtained from the generated output, the available power would
be least with the lower figures on the potentiometer were the
greatest. (See Fig. XXXVI). Thus the accuracy of control
power required for variable regulation is provided by
inserting by Eqn. XXXVI and XXXVII, in which the control
winding is used to maintain constant terminal voltage for
(1) variable power consumption by the load, and (2)
variable generator speed from 2,000 RPM to 12,000 RPM.

The control of terminal voltage under all load
conditions, and with variations in prime mover speed appears

FIGURE XVIII

GRAPHICAL SOLUTION

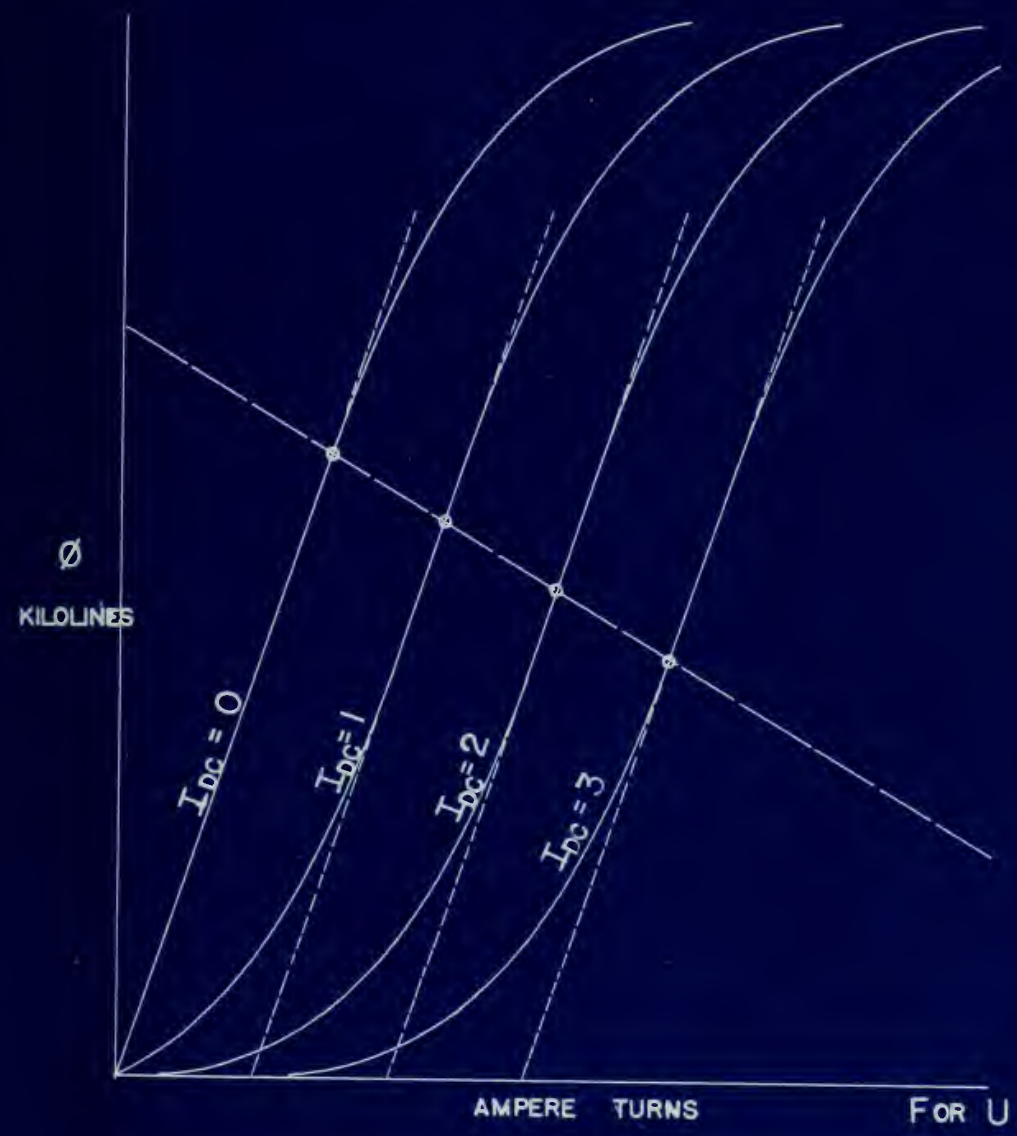

to be a highly valuable feature and should find wide application in systems which can use permanent magnet generators to advantage. Since the control is by purely electrical means, automatic voltage regulation is feasible.

The wave shape of the terminal voltage of a properly designed stator appears to remain constant, except in amplitude, throughout the range of control current used. Observations were made on an oscilloscope so minor changes in shape may not have been discerned. The saturation of the stator by control current does not have any effect on the stator teeth since all flux induced by the toroidal control winding must be contained within the toroid; thus, the condition of the iron in the stator teeth immediately opposite the permanent magnet poles is unchanged by control current. The air gap in the generator was only 0.007" so little air gap flux redistribution results as the control current increases. For these reasons, the effect of saturation of the stator iron will not have as much effect on the voltage wave shape as might first be suspected. On a machine with a larger air gap, some variation in the output voltage wave shape might well be observed.

Analysis and experiment both indicate that the stator magnetic material has little effect on the voltage control. This is because the point of intersection of the stator magnetic characteristic curve and the permanent magnet characteristic in the graphical solution occurs in the non-saturated region of the stator characteristic. That is,

the stator is not saturated due to the flux from the permanent magnet. Since the magnetic characteristics of materials suitable for use in generator stators are practically the same in the unsaturated condition, the graphical solution of the problem does not change.

Had the stator been saturated by the flux from the permanent magnet, the type of magnetic material would have marked effect on the initial voltage and the voltage control. The regulation obtained when the stator is originally saturated is marginal until the control current is increased enough to cause the stator to operate in an unsaturated condition. Figure XIX illustrates this effect.

The leakage path seen by the permanent magnet rotor has an effect of major importance on the reduction of air gap flux. The permanent magnet flux solved for as shown in Fig. XV does not represent the air-gap flux which actually induces voltage in the generator windings; leakage flux must be deducted from the permanent magnet flux to obtain air gap flux. The larger the leakage, the more reduction in air-gap flux per unit change in control current can be obtained. That the leakage was underestimated in the calculated results is evident from curve of Fig. XXXI. A method of improving the control obtained is to increase the available flux leakage paths. The effects of decreasing the reluctance of the leakage path facing the magnet is remarkably well demonstrated in Fig. XXXII.

To obtain these curves, several experiments were run

FIGURE XIX

EFFECT OF SATURATION IN THE STATOR BEFORE APPLICATION OF CONTROL MMF

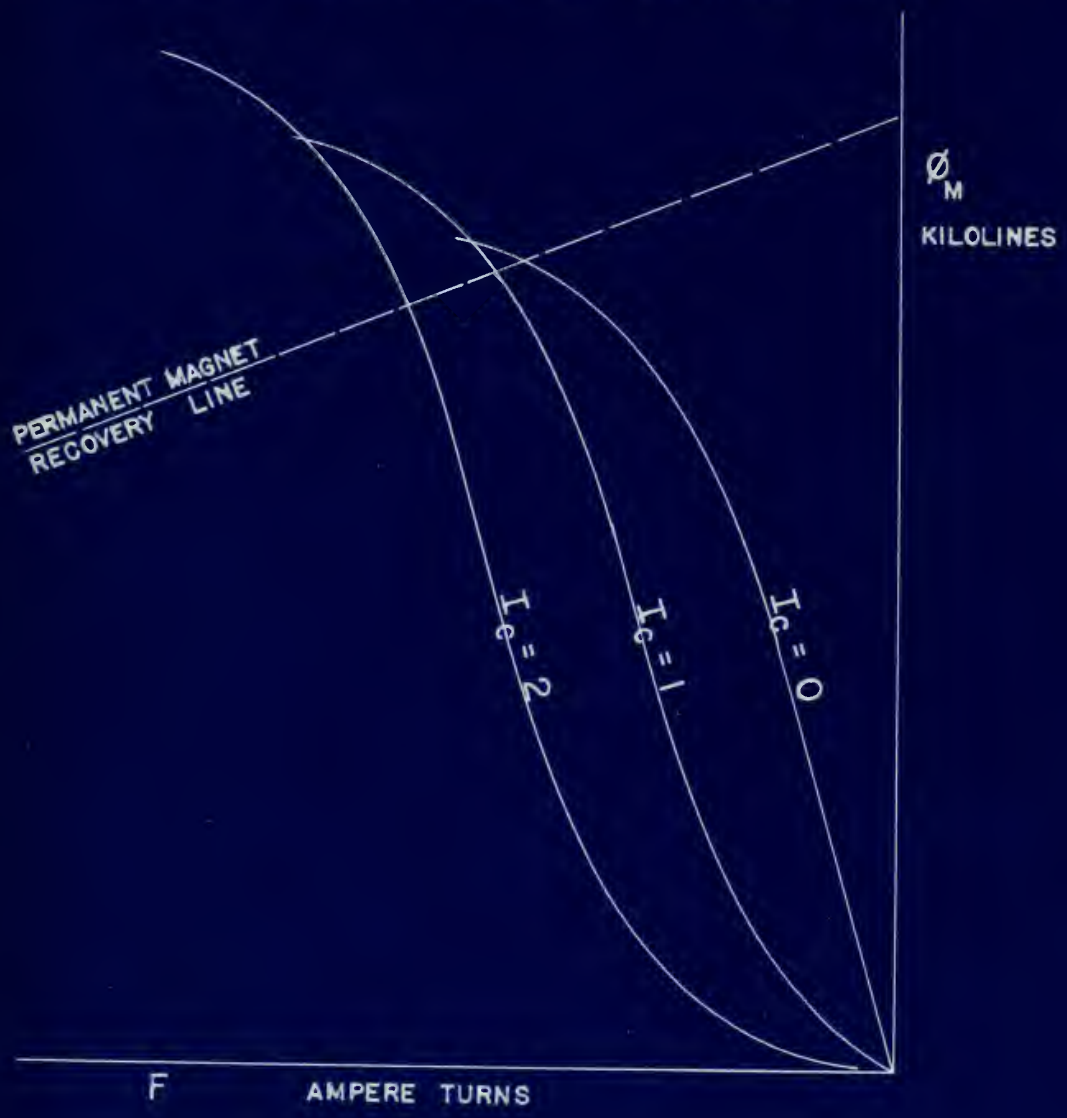

with magnetically soft discs separated from the rotor by non-magnetic spacers clamped to both ends of the rotor. It was found that increasing the leakage path by this auxiliary means did increase the per cent voltage regulation. The curves in Fig. XXXIIalso show that the voltage regulation eventually decreases at higher control currents because the leakage characteristic changes when the discs saturate. No analysis of this phase of the experiment was undertaken because of the uncertain nature of the auxiliary leakage path.

No trouble was encountered due to voltage being induced in the toroidal control winding since the north and south poles of the permanent magnet rotor induced equal and opposite voltages in this continuous winding.

with magnetically soft discs separated from the rotor by non-magnetic spacers clamped to both ends of the rotor. It was found that increasing the leakage path by this auxiliary means did increase the per unit voltage regulation. The curves in Fig. XXXIIIa show that the voltage regulation eventually decreases at higher control reactors because the leakage characteristic changes when the discs saturate. No analysis of this phase of the experiment was undertaken because of the uncertain nature of the auxiliary leakage path.

No trouble was encountered due to voltage being induced in the toroidal control winding since the north and south poles of the permanent magnet rotor induced equal and opposite voltages in this continuous winding.

V. CONCLUSIONS AND RECOMMENDATIONS

The method of analysis devised for the magnetic circuit under the specified conditions of saturation is sound in principle and leads to an acceptable prediction of resultant effects.

It has further been shown that this method is entirely practical for voltage control of a permanent magnet alternator by electrical means. The amount of control obtainable is limited only by the characteristics of the permanent magnet, the design of the magnetic circuit, and by the power one wishes to expend to obtain this control. One advantage of the permanent magnet alternator has, however, been lost. That is, now a source of direct current must be made available, and to obtain direct current from the output requires some rectifying mechanism or circuit.

The amount of control is greatly affected by the reluctance of the leakage paths, and the most obvious method of improving the control for a given power expenditure is to provide an easy leakage path in the magnetic circuit.

Recommendations for further investigation are as follows:

(1) Seek to improve the stator design to take advantage of the leakage effects to better advantage.

(2) Perform a more thorough study of the leakage paths to improve upon the approximations used in this analysis.

(3) Design a circuit for automatic voltage control of

the device, using rectified power from the output in a feedback loop. The transient characteristics and power characteristics would be of interest.

(4) Investigate the effects of alternating current at various frequencies applied to the toroidal winding.[6]

(5) Apply the principles learned herein to other types of machines where they may be of value. For example, poor voltage regulation of a high-speed induction generator is a serious disadvantage [7], [8]. This method of analysis suggests that the effects of toroidal saturation of an induction generator may be of interest.

VI. APPENDIX A

DETAILS OF PROCEDURE

VI. APPENDIX A

STATUS OF PROGRESS

DETAILS OF PROCEDURE

Machine Design:

The design is limited by the characteristics of the existing stator. The physical dimensions, the number of slots, and the shape of the laminations were left unchanged, and a three phase "Y" winding was designed which would generate approximately 90 volts per phase, root mean-square.

The peripheral rim was milled to produce 18 additional slots to recess the outside of the toroidal winding so it would clear the casing when the stator and case were assembled. See Fig. XX.

Design of the three-phase armature winding: [9]

The design of this winding is based upon two existing pieces of apparatus: the 18-slot stator and the permanent-magnet rotor.

The flux per pole is determined for the "closed circuit" position of the rotor (i.e.: rotor in place in the magnetic circuit) by the method outlined in Section II "PROCEDURE".

Flux per pole, $\phi_t = 21.7$ kilolines

Assume a field form distribution factor $f_d = 0.666$

Therefore the "hypothetical total flux" [9]:

$$\phi_t = \frac{\phi_p p}{f_d} = \frac{21.74\ (4)}{0.666} = 130.9 \text{ kilolines} \qquad (20)$$

$$B_g = \frac{\phi_t}{\pi D L} = \frac{130,900}{\pi\,(2.22.)(.875)} = 21520 \text{ lines/inch}^2 \qquad (21)$$

Machine Design:

The design is limited by the characteristics of the existing stator. The physical dimensions, the number of slots, and the shape of the insulations were fixed quantities, and a three phase "Y" winding was designed which would generate approximately 80 volts per phase, root mean-square.

The peripheral rim was milled to provide 18 additional slots to reduce the ripple of the voltage wave so it would place the cooling when the stator and rotor were assembled. See Fig. 12.

Design of the three phase armature winding: [3]

The design of this winding is based upon two existing pieces of apparatus: the 18-slot stator and the permanent-magnet rotor.

The flux per pole is determined for the "closed circuit" position of the rotor (i.e.: rotor in place in the magnetic circuit) by the method outlined in Section II "PROCEDURE".

Flux per pole, $\phi' = 17.7$ kilolines

Assume a field form distribution factor $k_d = 0.866$

Therefore the "apparent total flux" [3]:

$$\phi'_t = \frac{\phi'_p}{k_d} = \frac{17.74\ (\phi)}{0.866} = 230.3 \text{ kilolines} \qquad (19)$$

$$E_{ph} = \frac{\phi'_t}{10^5} = \frac{230,000}{\pi\,(3 \times 60)\,(4 \times 10)} = 81.50 \text{ lines/turn} \qquad (21)$$

FIGURE XX

DETAILS OF STATOR AND ROTOR

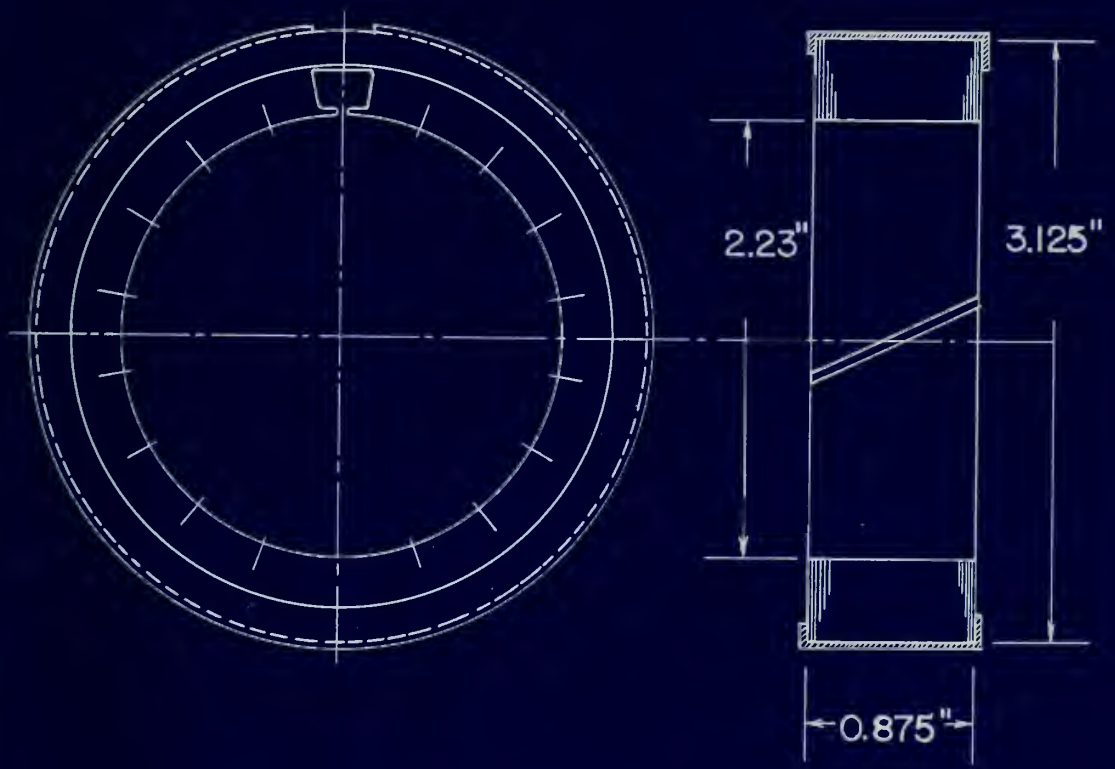

Assume a winding distribution factor C_w:

$$C_w = f_b \times f_d \times k_d \qquad (22)$$

$$= 1.14 \times 0.666 \times 0.956$$

$$= 0.725$$

Where f_b = form factor,

f_d = flux distribution factor

k_d = winding distribution factor

For a pitch winding, the number of conductors in series per phase N:

$$N = \frac{E \times 60 \times 10^8}{\phi_t \times n \times k_p \, C_w} = \frac{90 \times 60 \times 10^8}{130{,}900 \times 12{,}000 \times 1 \times 0.725} \qquad (23)$$

= 476 conductors in series per phase

The total number of conductors equals 476 x 3 = 1428 for a winding with one circuit per phase.

The number of conductors per slot is N.

$$N = 1428/18 = 79.2 \qquad (24)$$

However with this stator a pitch coil cannot be used, since the pitch equals $4\frac{1}{2}$ slots.

Therefore a coil throw of slots 1 to 5 will be necessary:

$$k_p = \sin\left[\frac{4}{4\frac{1}{2}} \times 90^\circ\right] = .986 \qquad (25)$$

Assume a winding distribution factor C_d^3:

$$C_d^3 = t_p^3 \times t_d^3 \times k_d^3 \qquad (28)$$

$$= 1.19 \times 0.809 \times 0.996$$

$$= 0.959$$

Where t_p^3 = form factor,

t_d^3 = flux distribution factor

k_d^3 = winding distribution factor

For a pitch winding, the number of conductors in series per phase S:

$$S = \frac{3 \times 60 \times 10^6}{p^3 \times n \times \phi^3 \times C_d^3} = \frac{90 \times 60 \times 10^6}{120^3 \times 200 \times 11,000 \times 1 \times 0.959} \qquad (29)$$

= 456 conductors in series per phase

The total number of conductors equals 456 x 3 = 1368

for a winding with one circuit per phase.

The number of conductors per slot is S.

$$S = 1368/216 = 6.3 \qquad (30)$$

Suppose with this winding a pitch coil common to slots,

since the pitch equals 6 slots.

Therefore a coil throw of slots 1 to 7 will be

necessary:

$$k^3 = \sin\left[\frac{\pi^3}{2} \times 30^\circ\right] = .966 \qquad (31)$$

and $N = \frac{476}{.986} = 483$ conductors in series per phase. (26)

The total number of conductors = 483 x 3 = 1449

Therefore we will have $\frac{1449}{18} = 80.3 \approx 80$ conductors per slot, or 40 turns per coil.

Figure XXI shows the wiring diagram for the three-phase winding, and Fig. XXII shows the coil end-connections.

Wire size; and machine rating:

Determination of wire size depends upon space considerations in the slots.

Stator Number 1 (USS Electrical Steel) was limited to 40 turns per coil of Number 26 gauge wire.

S_a = cross sectional area of wire

S_a = .000199 square inches

A_a = allowable current density for short term operation

= 4400 amperes per square inch (twice normal)

I_a = allowable armature current

$= S_a \times A_a = (.000199) \times (4400) = .875$ amperes. (27)

Machine rating:

$VA = 3 E I_a = 3 \times 90 \times .875 = 236.2$ volt-amperes. (28)

Stator Number 2 ("HIPERNIK"): In this stator the absence of skew gave more effective slot area, allowing Number 24 gauge wire to be used.

and $X = \frac{1440}{1440} = 0.9$ conductors in service per phase. (20)

The total number of conductors = 980 x 3 = 1440

Therefore we will have $\frac{1440}{18}$ = 80.3 ≈ 80 conductors

per slot, or 40 turns per coil.

Figure XXI above the winding diagram for the three-

phase winding, and Fig. XXII above the coil end-connections.

Wire sizes and working voltage:

Determination of wire size depends upon three

considerations in the slots.

Stator Number 1 (USE Electrical Steel) was limited to

40 turns per coil of Number 26 Enamel wire.

S^a = cross sectional area of wire

S^a = .000159 square inches

A^a = allowable current density for short term operation

= 4400 amperes per square inch (basis normal)

I^a = allowable maximum current

$= S^a \times A^a = (.000159) \times (4400) = .873$ amperes, (21)

Working voltage:

$AV = 3 \times I^a = 3 \times 30 \times .873 = 250.5$ volt amperes. (22)

Stator Number 2 ("SUPERIOR"): In this wire-the

absence of slots gave more effective slot area, allowing

Number 24 Enamel wire to be used.

FIGURE XXI

DIAGRAM FOR THREE PHASE WINDING

1 1/2 SLOTS PER POLE PER PHASE

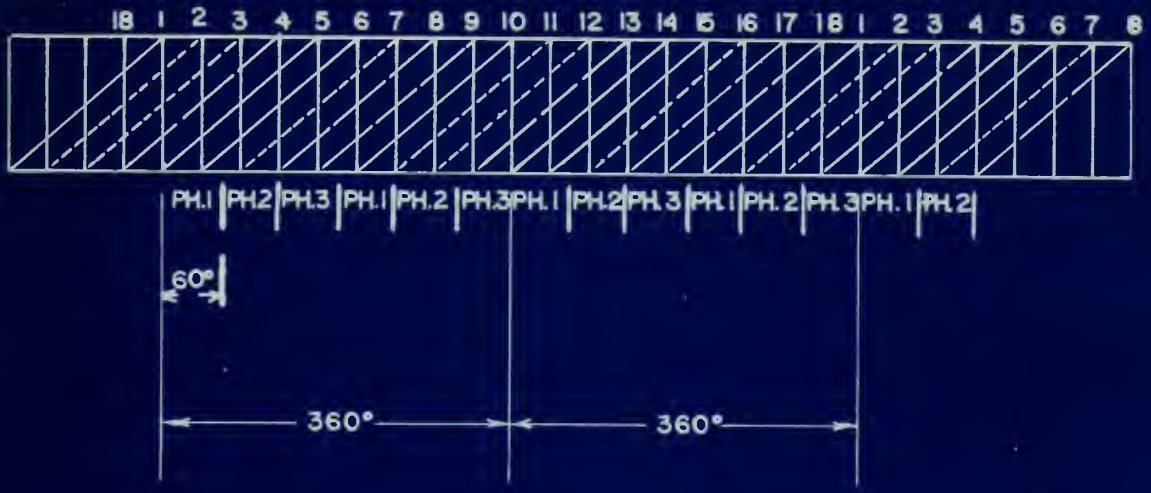

● PH. 1
⊖ PH. 2
○ PH. 3

FIGURE XXII

GENERATOR COIL END CONNECTIONS

THREE PHASE — Y CONNECTED

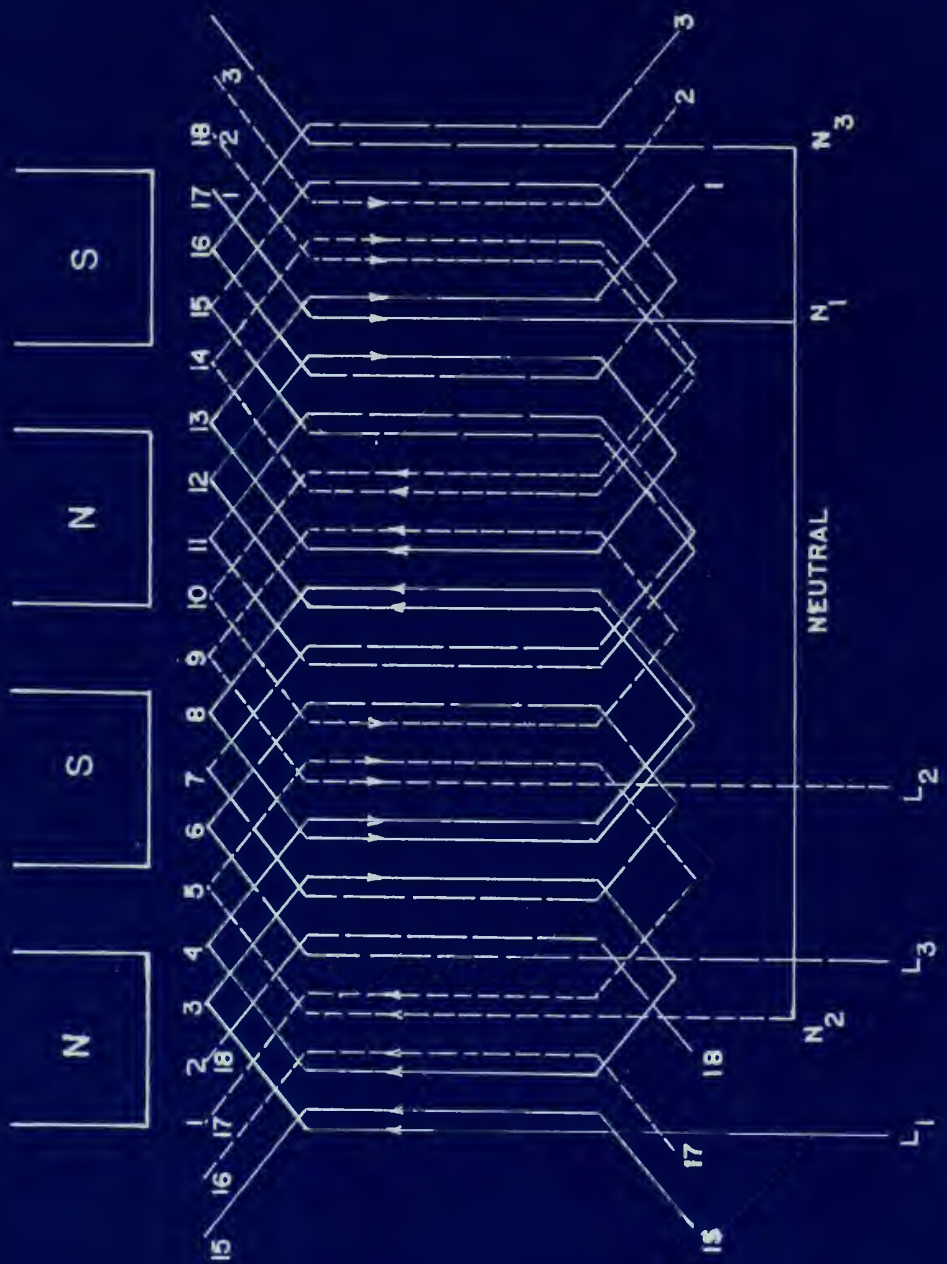

S_a = .000317 square inches

A_a = 4400 amperes per square inch

$I_a = S_a \times A_a = (.000317) \times (4400) = 1.395$ amperes (29)

Machine rating:

$VA = 3 E I_a = 3 \times 90 \times 1.395 = 377$ volt-amperes (30)

(cont.) EXERCISES ON ELECTRICITY

Details of "Shearing": [5]

A method of obtaining the reluctance characteristics of a magnetic path consisting of a ferromagnetic portion plus an air gap in series is as follows: Neglecting leakage, the flux may be assumed constant throughout the magnetic circuit. Then on coordinates of flux versus magnetomotive force (or magnetic potential drop U) we can plot separately the characteristics of the air gap and the rest of the circuit, as shown in Fig. XXIII.

Then, since these two portions of the magnetic circuit are in series, for each value of flux (Ø) the magnetic potential drop (U) of the entire circuit is the sum of the magnetic potential drops of the two portions. This addition may be done graphically by a process known as "shearing" the characteristic of the ferromagnetic portion into the air-gap line as shown in Fig. XXIV.

Details of "Separation" [2]

A method of obtaining the relationship characterizing
of a magnetic path containing an air gap is given
plus an air gap is entered in the first. Neglecting
leakage, the flux may be assumed constant through-out the
magnetic circuit. Then on considering or flux density
magnetomotive force (or magnetic potential drop U) we can
plot separately the characteristics of the air gap and the
rest of the circuit, as shown in Fig. XXIII.

Then, since these two portions of the magnetic circuit
are in series, for each value of flux (M) the magnetic
potential drop (U) of the entire circuit is the sum of the
magnetic potential drops of the two portions. This
addition may be done graphically by a process known as
"shearing" the characteristic of the ferromagnetic portion
into the air-gap line as shown in Fig. XXIV.

FIGURE XXIII

SAMPLE CHARACTERISTICS OF IRON & AIR GAP

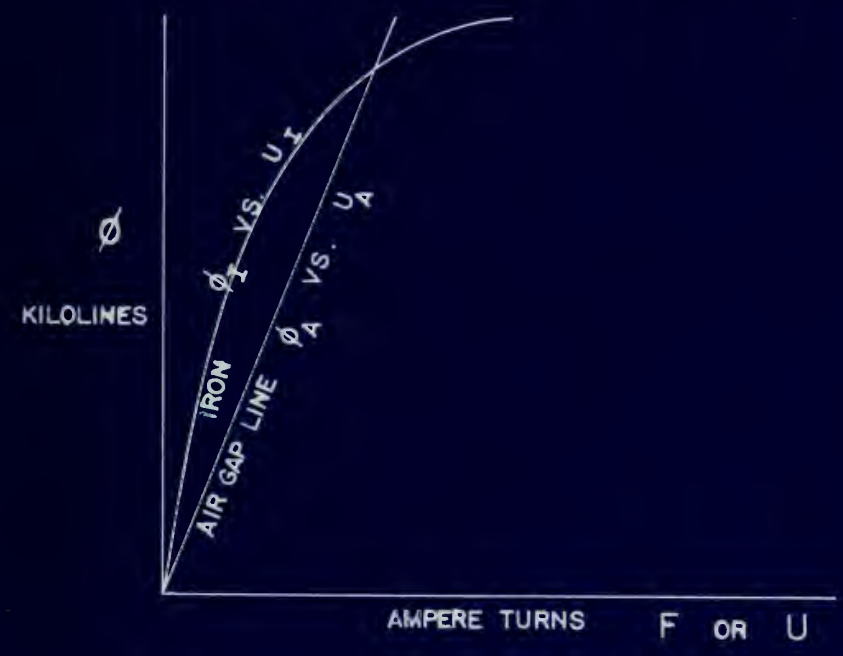

FIGURE XXIV

SHEARING

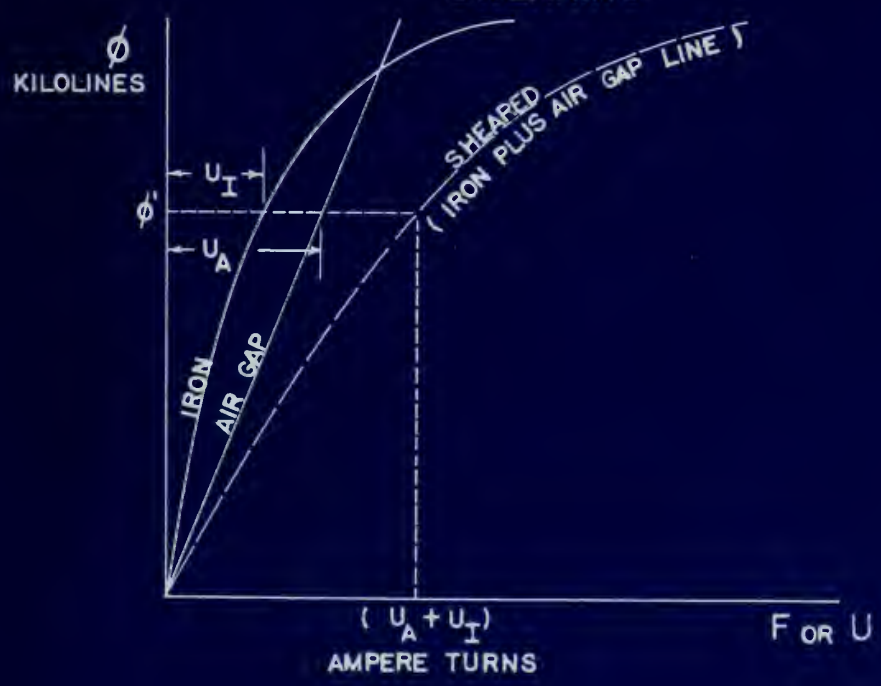

Computation of Air-Gap Line:

The dimensions of the armature iron and permanent magnet rotor are as shown in Fig. XX.

The air gap between pole face and stator teeth is:

$$a\text{-}g = r_i - r_m = 1.115" - 1.108" = 0.007" \qquad (31)$$

The true air-gap cannot be used directly for computation of the air-gap line in flux vs. magnetomotive force because of the effect of slot openings in the stator. An approximation of an effective air-gap; that is, a fictitious air-gap which would be required if the inside of the stator were made perfectly smooth and the air-gap adjusted so that the flux from the rotor were not changed, is made by the method of Carter [5].

The method of Carter is based on the assumption of slot openings with straight sides and with infinite depth. In the case of the slots under consideration, the slots are semi-closed, not straight, but the method is used on the assumption that the fringing flux will be about the same whether the slots be open or semi-closed since the depth at the edge of a slot tooth is over five times the air gap. This assumption neglects any saturation in the thin parts of the teeth.

Carter's method is outlined below:

$$\sigma = \frac{2}{\pi}\left\{\mathrm{Tan}^{-1}\frac{s}{2\delta} - \frac{\delta}{s}\mathrm{Ln}\left[1+\left(\frac{s}{2\delta}\right)^2\right]\right\} \qquad (32)$$

$$C = \frac{t+s}{t+s(1-\sigma)} \qquad (33)$$

$$\delta' = C\delta \qquad (34)$$

Computation of Air-Gap Lines:

The dimensions of the armature iron and permanent magnet rotor are as shown in Fig. XI.

The air gap between pole face and stator teeth is:

$$g = r_1 - r_2 = 1.113" - 1.108" = 0.005" \qquad (31)$$

The true air-gap cannot be used directly for computation of the air-gap line in flux vs. magnetomotive force because of the effect of slot openings in the stator. An approximation of an effective air-gap; that is, a fictitious air-gap which would be replaced if the insides of the stator were made perfectly smooth and the air-gap adjusted so that the flux from the rotor were not changed, is made by the method of Carter [3].

The method of Carter is based on the assumption of slot openings with straight sides and with infinite depth. In the case of the slots under consideration, the slots are semi-closed, not straight, but the method is used on the assumption that the crowding flux will be about the same whether the slots be open or semi-closed since the depth at the edge of a slot tooth is over five times the air gap. This assumption neglects any saturation in the thin parts at the teeth.

Carter's method is outlined below:

$$g' = Cg \qquad (32)$$

$$C = \frac{t + 5(1-\alpha)}{t + 5} \qquad (33)$$

$$\alpha = \frac{4}{5\pi}\left\{\tan^{-1}\frac{5b}{2g} - \frac{1}{2}\ln\left[1+\left(\frac{5b}{2g}\right)^2\right]\right\} \qquad (34)$$

where:

s = width of opening between teeth
δ = air-gap length
σ = an intermediate factor
t = length of tooth face
C = Carter coefficient, the ratio between effective air-gap and actual air-gap
δ' = effective air gap

$$\sigma = \frac{2}{\pi}\left\{\text{TAN}^{-1}\frac{0.05}{2 \times 0.007} - \frac{0.007}{0.05}\,\text{Ln}\left[1 + \left(\frac{0.05}{2 \times 0.007}\right)^2\right]\right\} = 0.594 \tag{35}$$

$$C = \frac{0.34 + 0.05}{0.34 + 0.05\ (1-0.594)} = 1.082 \tag{36}$$

$$\delta' = 1.082 \times 0.007 = 0.00758" \tag{37}$$

The area of each pole face, corrected for air-gap fringing is:

$$A = (l_m + \delta')(l_f + \delta') = (0.875 + 0.0076)(1.156 + 0.0076) \tag{38}$$

$$= 1.03 \text{ in}^2 \tag{39}$$

The length of two air gaps in series is:

$$2 \times 0.00758 = 0.0152" \tag{40}$$

The slope of the air-gap line is:

$$\frac{\phi}{F} = \frac{\mu_o A}{2\delta'} \tag{41}$$

where: μ_o = the permeability of free space
= 3.192 in mixed English units

$$\frac{\phi}{F} = \frac{3.192 \times 1.03}{0.0152} = 216\ \frac{\text{Lines}}{\text{Amp-Turn}} \tag{42}$$

Estimate of Flux Leakage

Leakage flux can be estimated by several methods [6], but in any case the estimate should be checked by actual experiment. For an approximation of the slope of the leakage line, the reluctance of the stator iron is neglected. The short air-gap between the rotor and stator is neglected because the area of this air gap in series with the leakage path cannot be determined and is small compared to the remainder of the leakage path. Only the reluctance in the air between the edges of the teeth is considered as shown in Fig. XXV.

Assume, due to fringing, the area of the gap between teeth edges is twice the area of the edge of a tooth.

The leakage flux of the USS Electrical Grade stator will not be the same as that of the HIPERNIK stator because the former has a slot skew of one slot pitch between stator ends whereas the latter stator has no skew.

For the skewed stator, referring to the dimensions shown in Fig. XX, the length of a tooth edge is:

$$\ell = \sqrt{(0.875)^2 + (0.34 + 0.05)^2} = 0.958 \qquad (43)$$

The leakage line is:

$$\frac{\phi}{F} = \frac{3.192 \times 0.958 \times 0.04 \times 2}{0.05} = 4.9 \quad \frac{\text{Lines}}{\text{Amp-Turn}} \qquad (44)$$

Since the rotor sees two of these paths in parallel, the slopes of the leakage line is:

$$\frac{\phi}{F} = 2 \times 4.9 = 9.8 \quad \frac{\text{Lines}}{\text{Amp-Turn}} \qquad (45)$$

Reliable of Flux Leakage

Leakage flux can be estimated by several methods [6], but in any case the estimate should be checked by actual experiment. For an approximation of the slope of the leakage line, the reluctance of the stator iron is neglected. The short air-gap between the rotor and stator is neglected because the area of this air gap is small compared to the remainder of the leakage path. Study the relations in the air between the edges of the teeth is considered as shown in Fig. 32A.

Assume, due to fringing, the area of the gap between teeth edges is twice the area of the edge of a tooth.

The leakage flux of the 7HB Electrical Dynamo stator will not be the same as that of the EXPERIMENTAL stator because the former has a slot width of one slot pitch between stator ends whereas the latter stator has no skew.

For the skewed stator, referring to the dimensions shown in Fig. 32, the length of a tooth edge is:

$$\lambda = \sqrt{(0.375)^2 + (0.75 + 0.05)^2} = 0.975 \qquad (42)$$

The leakage line is:

$$\frac{\ell}{\rho} = \frac{3.125 \times 0.975 \times 0.94 \times 2}{0.05} = 4.9 \quad \frac{\text{Kilomax}}{\text{Amp-Turn}} \qquad (44)$$

Since the rotor area is two of these parts in parallel, the slope of the leakage line is:

$$\frac{\ell}{\eta} = 2 \times 4.9 = 9.8 \quad \frac{\text{Kilomax}}{\text{Amp-Turn}} \qquad (45)$$

In addition to leakage between teeth edges, the skewed stator has another leakage path due to a tooth in the gap between adjacent poles which partially overlaps each of the adjacent pole faces as shown by the shaded areas in Fig. XXVI.

The area of each of the triangular shaped air gaps (which are in series) is:

$$A = \tfrac{1}{2}\left(\tfrac{1}{4}t\right)\left(\tfrac{1}{4}l_i\right) = \tfrac{1}{32}(0.34)(0.875) = 0.0093 \text{ in}^2 \qquad (46)$$

and

$$\frac{\phi}{F} = \frac{3.192 \times 0.0093}{2 \times 0.007} = 2.12 \quad \frac{\text{Lines}}{\text{Amp-Turn}} \qquad (47)$$

This leakage path can occur only between one pair of adjacent poles at one time; that is, the value $\frac{\phi}{F} = 2.12$ is not doubled since there is no similar path at the other edge of a pole at any one instant.

The total slope of the leakage line for the skewed stator is

$$\frac{\phi}{F} = 9.8 + 2.12 = 11.92 \quad \frac{\text{Lines}}{\text{Amp-Turn}} \qquad (48)$$

since the slopes 2.12 and 9.8 are added as paralleled circuit elements.

For the stator without skew, the slope of the leakage line is considered to be:

$$\frac{\phi}{F} = (2)\ \frac{3.192 \times 0.875 \times 0.04 \times 2}{0.05} = 8.94 \ \frac{\text{Lines}}{\text{Amp-Turn}} \qquad (49)$$

In addition to locating intrinsic zeros, the above subroutine locates singular points due to a touch in the two nearest adjacent poles which partially overlaps each of the adjacent pole zones as shown by the circles drawn in Fig. XXVI.

The area of each of the triangular pieces are

(which are in series) in:

$$A = \frac{1}{2}\left(\frac{1}{4}f\right)\left(\frac{1}{4}h\right) = \frac{1}{32}[0.34][0.57] = 0.0093 \text{ in}^2 \qquad (46)$$

and

$$\frac{R}{P} = \frac{2.126 \times 0.0093}{2 \times 0.057} = 0.17 \qquad \frac{\text{Amp-Turns}}{\text{Amp-Turns}} \qquad (47)$$

This Impulse pair was found only in the case of adjacent poles as the other case in Fig. XXV the value $\frac{R}{P} = 0.32$ is not doubled since there is no mutual path as the other half of a pole at 60° was included.

The total slope of the Impulse line for the assumed example is

$$\frac{R}{P} = 3.5 + 0.17 = 13.5 \qquad \frac{\text{Amp-Turns}}{\text{Amps}} \qquad (48)$$

since the slopes 9.12 and 3.5 are added as previously circuit elements.

For the exact solution when, the slope of the Impulse line is computed in the:

$$\frac{R}{P} = (0) \quad \frac{2.126 \times 0.057 \times 12.84 \times 2}{0.06} = 0.84 \quad \frac{\text{Amp-Turns}}{\text{Amps}} \qquad (49)$$

FIGURE XXV

PATH ASSUMED FOR LEAKAGE COMPUTATIONS

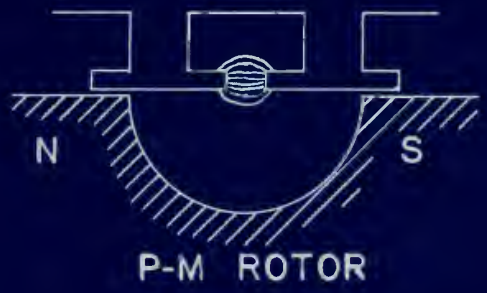

FIGURE XXVI

DEVELOPED SECTION OF STATOR

SHOWING LEAKAGE PATH ALONG LENGTH OF ONE TOOTH DUE TO SLOT SKEW

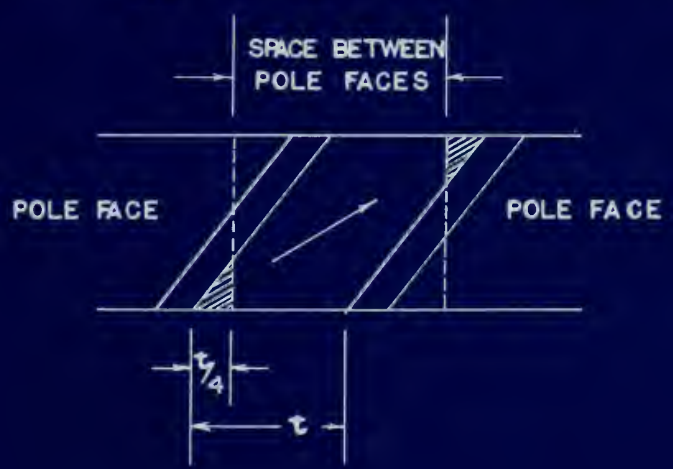

VI. APPENDIX B

DETAILS OF CALCULATED DATA

VI. APPENDIX B

DETAILS OF TABULATED DATA

DETAILS OF CALCULATED DATA

TABLE I

Plot of the demagnetization curve of Alnico VI in terms of flux and Magnetomotive force

Flux Density (kilogauss) B	Flux ϕ_m (kilolines) BA x 6.45	Magnetizing Force H: (amp-turns/in.)	Magnetomotive Force, F, or Mag. Potential difference U. (amp-turns) H x L_m H x 2.78"
10.3	67.3	0	0
9.98	65.2	100	278
9.50	62.0	200	556
8.99	58.65	300	833
8.20	53.60	400	1113
7.05	46.00	500	1390
5.20	34.0	600	1669
3.75	24.5	650	1807
2.00	13.05	700	1945
0.0	0.0	750	2085

TABULATION OF CALCULATED DATA

TABLE I

Flow of the downstream/slow curve of Alpha VI in terms of flux and pressure drop

DETAILS OF CALCULATED DATA (cont.)

Plot of magnetization curve of USS Electrical Steel in terms of flux and magnetic potential drop:

Flux density (Kilogauss) multiplied by effective cross section and a conversion factor 6.45 equals flux in kilolines:

$$\phi = B \times A \times 6.45 = B \times .156 \times 6.45 \qquad (50)$$

Magnetizing force H (Oersteds) multiplied by the length of the magnetic path and the conversion factor 2.01 equals magnetic potential drop U in ampere turns:

$$U = H \times L \times 2.01 = H \times 2.25 \times 2.01 \qquad (51)$$

TABLE II

26 Gauge USS Electrical

ø (kilolines)	U (amp-turns)
0	3.15
4.68	4.28
6.24	4.73
7.80	6.30
9.36	7.20
10.92	11.25
11.70	14.25
12.50	21.6
13.26	32.6
14.05	54.0
14.82	88.9
15.60	157.6
16.39	239
17.18	446
17.95	619

Plot of magnetization curve of the Electrical Steel in terms of flux and magnetic potential drop.

Flux density (kilogauss) multiplied by effective cross section and a conversion factor 6.45 equals flux in kilolines.

$$\Phi = B \times A \times 6.45 = B \times .706 \times 6.45 \quad \ldots\ldots (34)$$

Magnetizing force H (Oersteds) multiplied by the length of the magnetic path and the conversion factor 1.01 equals magnetic potential drop U in ampere turns.

$$U = H \times L \times 1.01 = H \times 8.25 \times 1.01 \quad \ldots\ldots (35)$$

TABLE II

DC Curve for Electrical

Φ (kilolines)	U (amp-turns)
6	3.45
6.85	4
7.4	4.73
7.85	5.49
8.24	6.29
8.56	7.08
8.85	7.88
9.14	8.68
9.42	9.48
9.69	10.28
9.96	11.08
10.22	11.89
10.48	12.69
10.74	13.49
10.99	14.29
11.24	15.09
11.49	15.89
11.74	16.69
11.99	17.49
12.24	18.29
12.49	19.09
12.74	19.89
12.99	20.69
13.24	21.49
13.49	22.29
13.74	23.09
13.99	23.89
14.24	24.69
14.49	25.49
14.74	26.29
14.99	27.09
15.24	27.89
15.49	28.69
15.74	29.49
15.99	30.29
16.24	31.09
16.49	31.89
16.74	32.69
16.99	33.49
17.24	34.29
17.49	35.09
17.74	35.89
17.99	36.69
18.24	37.49
18.49	38.29
18.74	39.09
18.99	39.89
19.24	40.69
19.49	41.49
19.74	42.29
19.99	43.09

DETAILS OF CALCULATED DATA (cont.)

TABLE III

Magnetic Circuit Dimensions

Area of magnet pole-face = 1.011 sq. in.

Minimum area of stator path = 0.156 sq. in.

Length of mean rotor flux path = 2.78 inches.

Length of air gap = 0.007 inches (at each pole face)

Total effective length of air gap = 0.0154 inches

Length of stator (saturable) path = 2.25 inches

DETAILED DESIGN CALCULATIONS (cont.)

TABLE III

Magnetic Circuit Dimensions

Area of magnet pole-face = 1.011 sq. in.

Minimum area of stator pack = 0.750 sq. in.

Length of mean rotor flux path = 2.78 inches.

Length of air gap = 0.007 inches (at each pole face)

Total effective length of air gap = 0.015 inches

Length of stator (saturable) pack = 1.35 inches

DETAILS OF CALCULATED DATA (cont.)

TABLE IV

Plot of the magnetization curve of HIPERNIK in terms of flux and magnetic potential drop

Conversion factors same as on previous page:

B (Kilogauss)	∅ (kilolines)	H (Oersted)	U (amp-turns)
0	0	0	0
9.6	9.65	0.2	.911
10.6	10.65	0.4	1.82
11.2	11.25	0.6	2.73
11.6	11.68	0.8	3.64
11.9	11.98	1.0	4.55
12.1	12.18	1.2	5.56
15.2	15.29	20.0	91.1
15.75	15.85	40.0	182.0
15.85	15.95	60.0	273
15.9	16.0	80.0	364
16.0	16.09	100.0	455

TABLE IV

Plot of the magnetization curve of DYSPROSIA in terms of FLUX AND MAGNETIC POTENTIAL DROP

Commercial Ferrite rods as the previous Paper

B (Kilogauss)	H (Oersted)	H (Oersted)	B (Kilo-Gauss)
0	0	0	0
9.8	9.85	9.2	1.21
10.8	10.85	8.4	1.89
11.4	11.35	6.4	2.73
12.0	11.88	4.8	3.69
12.9	12.98	1.4	4.95
13.1	13.18	1.2	5.58
15.4	15.34	30.6	21.1
15.75	15.85	40.6	180.6
15.85	15.95	60.6	272
15.9	16.0	80.6	364
15.9	16.34	100.6	454

DATA

TABLE V

DETAILS OF STATORS

STATOR NO. 1:

Material:	USS Electrical Grade Steel, 0.014" Laminations
Toroidal Winding:	9 turns per slot, 162 total turns, #24 wire 0.96 ohms cold 4.4 millihenries
Three-phase Winding:	40 turns per coil of #29 wire Line to line Resistance: 23.4 ohms (cold) Skewed one slot pitch

STATOR NO. 2:

Material:	Hipernik, annealed in Hydrogen atmosphere
Toroidal Winding:	11 turns per slot, 198 turns total, #24 wire 1.11 ohms (room temperature) 16 millihenries
Three-phase Winding:	40 turns per coil of #26 wire Line to line resistance: 11 ohms (Rm. Temp) 9.5 millihenries No skew

In both stators the length of the magnetic path was assumed to be 2.25 inches, and the cross sectional area 0.156 square inches.

FIGURE XXVII
GRAPHIC SOLUTION

STATOR NO. 1 - USS ELECTRICAL

ALNICO VI ROTOR

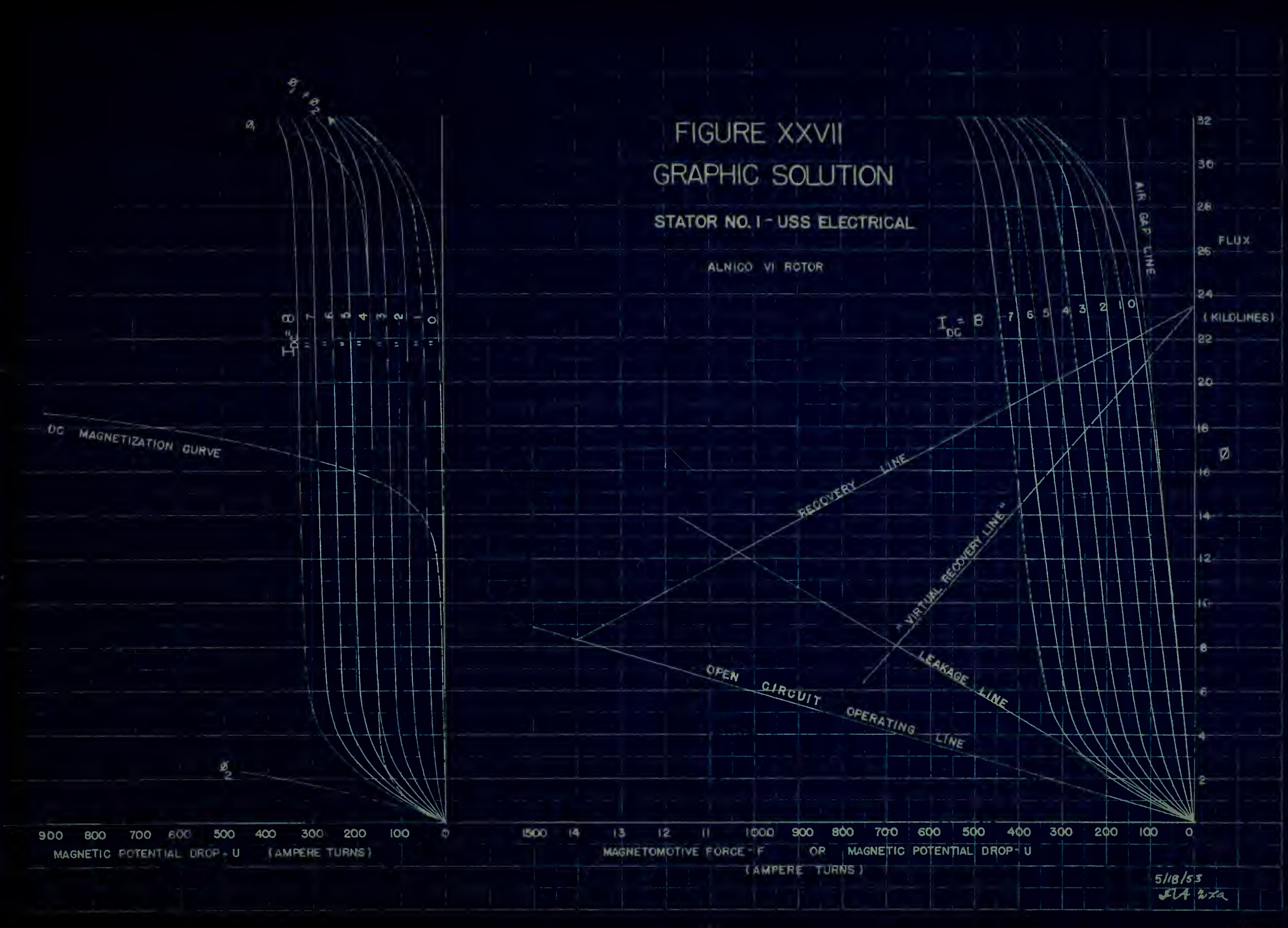

5/18/53
JLA 2xa

FIGURE XXVIII
GRAPHIC SOLUTION
STATOR NO. 2 - HIPERNIK
ALNICO VI ROTOR

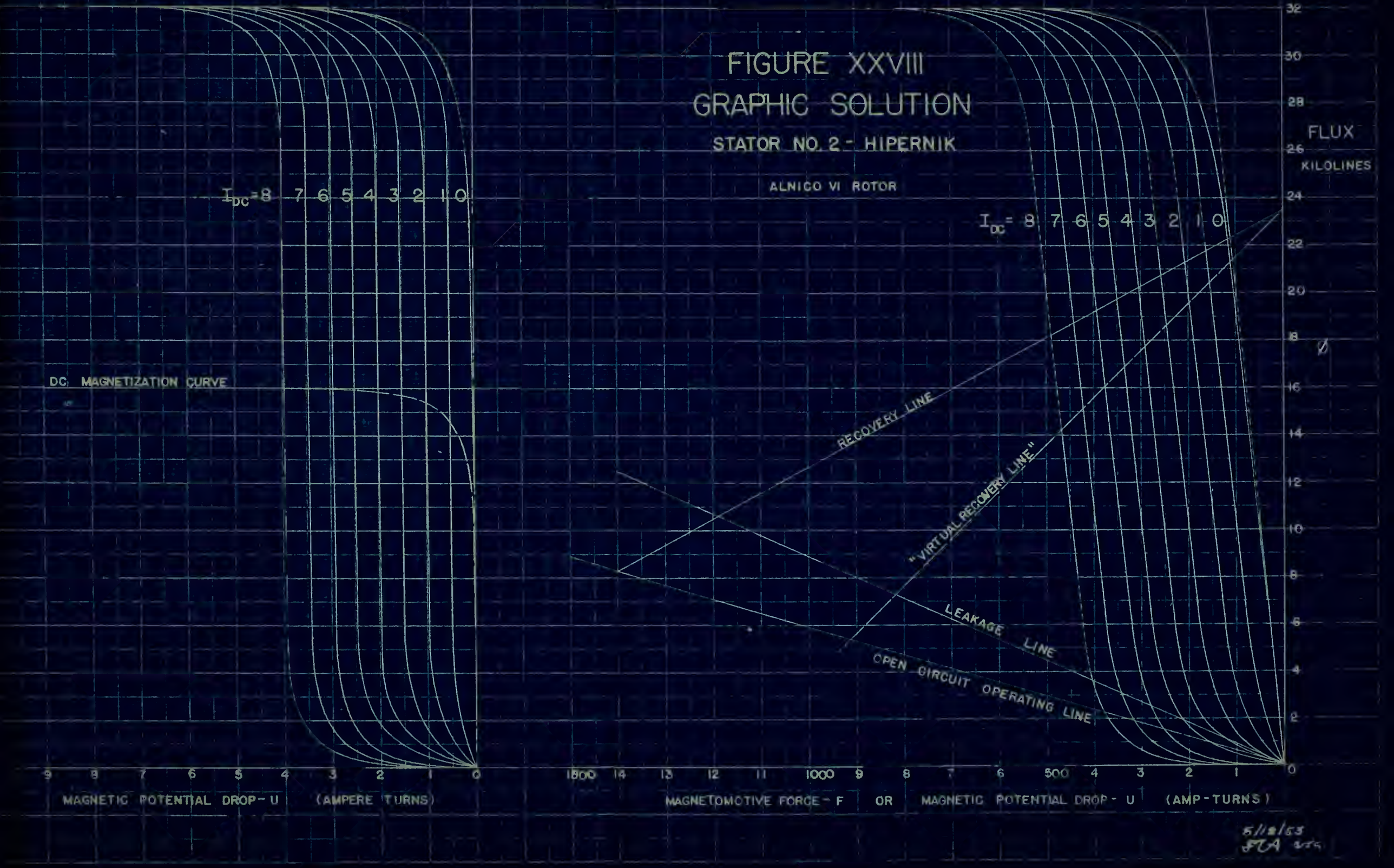

5/18/53
SCA ats

VI. APPENDIX C

SUMMARY OF DATA AND CALCULATIONS

72. APPENDIX C

GLOSSARY OF TERMS AND CALCULATIONS

SUMMARY OF DATA AND CALCULATIONS

The summary of data and calculations is presented in the graphs following.

Figure XXIX:

This figure shows the percentage of initial voltage of the alternator as obtained both by theoretical means and by experiment. The stator laminations are of USS Electrical Grade Steel, and the stack is skewed one slot pitch. The dotted line is the theoretical curve as calculated by the method explained in Section II, "PROCEDURE". Experimental values obtained under various conditions of loading are shown and explained on the figure.

Figure XXX:

This figure is a summary of raw data for the HIPERNIK stator.

Figure XXXI:

This figure is similar to Figure XXIX, except that it represents analysis and experiment on a stator whose laminations are of HIPERNIK and whose slots have no skew. The loads are also slightly different as explained on the figure.

Figure XXXII:

This figure shows the comparison of voltage behavior with and without additional leakage paths being added to the magnetic circuit.

SUMMARY OF DATA AND EXPLANATIONS

The summary of data and explanations is presented in the pages following.

Figure XXII:

This figure shows the percentage of initial voltage of the alternator as obtained both by theoretical means and by experiment. The stator inductions are of THE Micrometrical Brush Sheet, and the study is shown one plot. The dotted line is the theoretical curve as calculated by the method explained in Section XI, "PROCEDURE". Experimental values obtained under various conditions of loading are shown and explained on the figure.

Figure XXX:

This figure is a summary of raw data for the SIEMENS stator.

Figure XXXI:

This figure is similar to Figure XXIX, except that it represents analysis and experiment on a stator whose inductions are of SIEMENS and whose slots have no skew. The loads are also slightly different as explained on the figure.

Figure XXXII:

This figure shows the comparison of voltage behavior with and without additional leakage paths being added to the magnetic circuit.

FIGURE XXIX

STATOR NO.1 - USS ELECTRICAL

PERCENT OF INITIAL VOLTAGE VS.
CONTROL MAGNETOMOTIVE FORCE

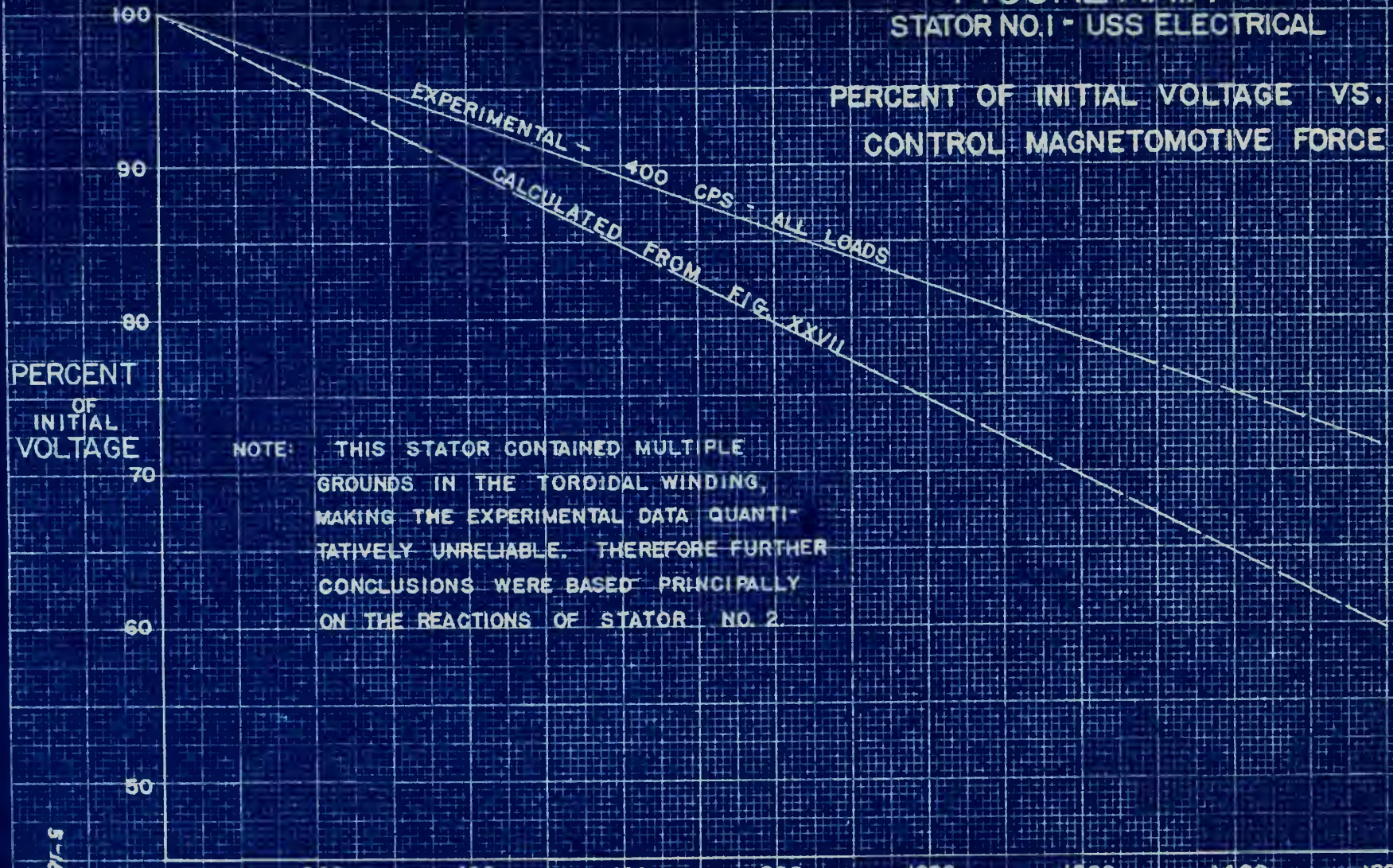

FIGURE XXIX

5-1/8-53 RCA W.L.A.

FIGURE XXX

STATOR NO. 2 - HIPERNIK

TERMINAL VOLTAGE VS. CONTROL MMF FOR VARIOUS LOADS

400 CPS

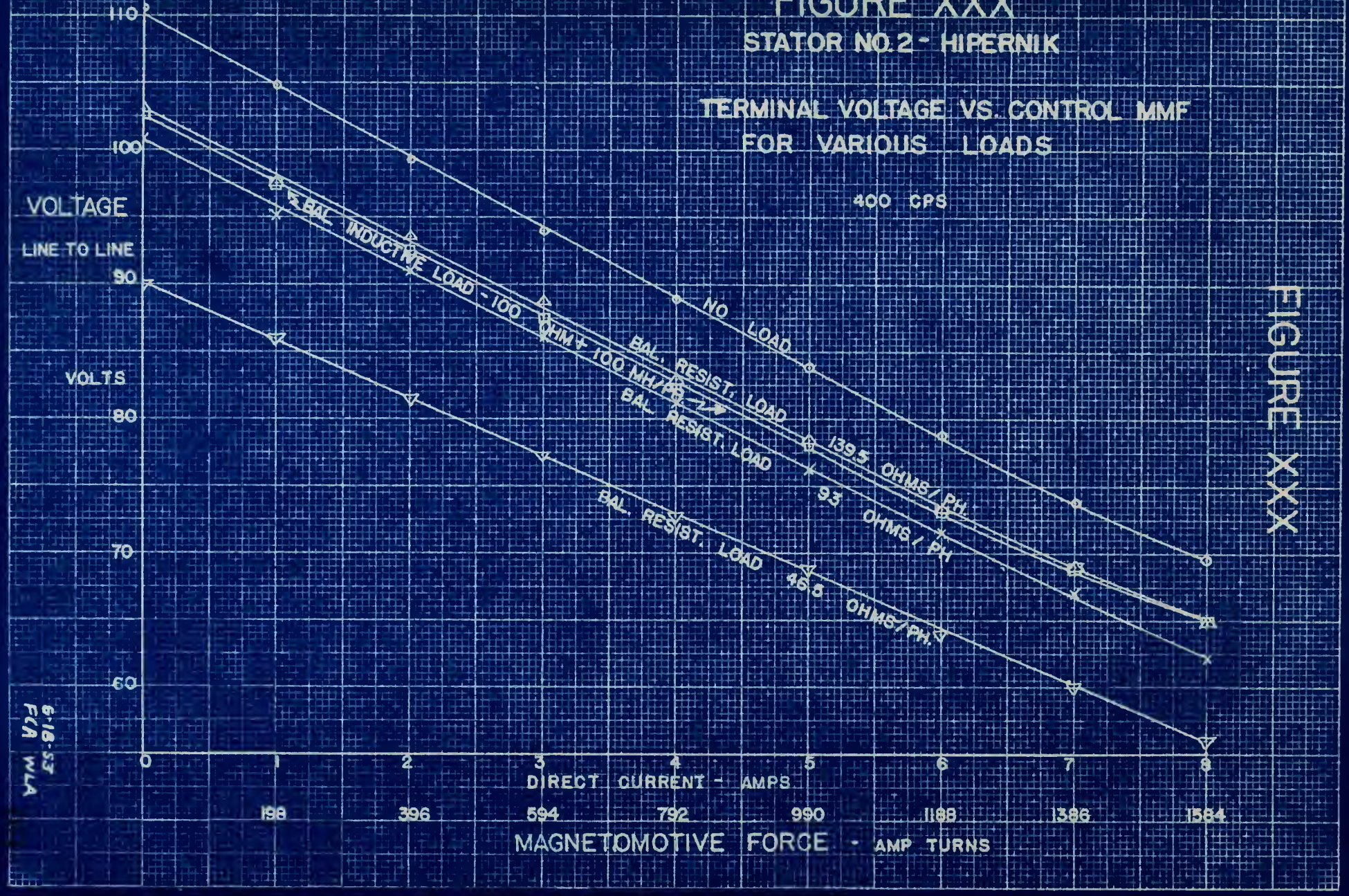

FIGURE XXX

6-18-37
F.A.
W.L.A.

FIGURE XXXI

STATOR NO. 2 - HIPERNIK

PERCENT OF INITIAL VOLTAGE VS CONTROL MAGNETOMOTIVE FORCE

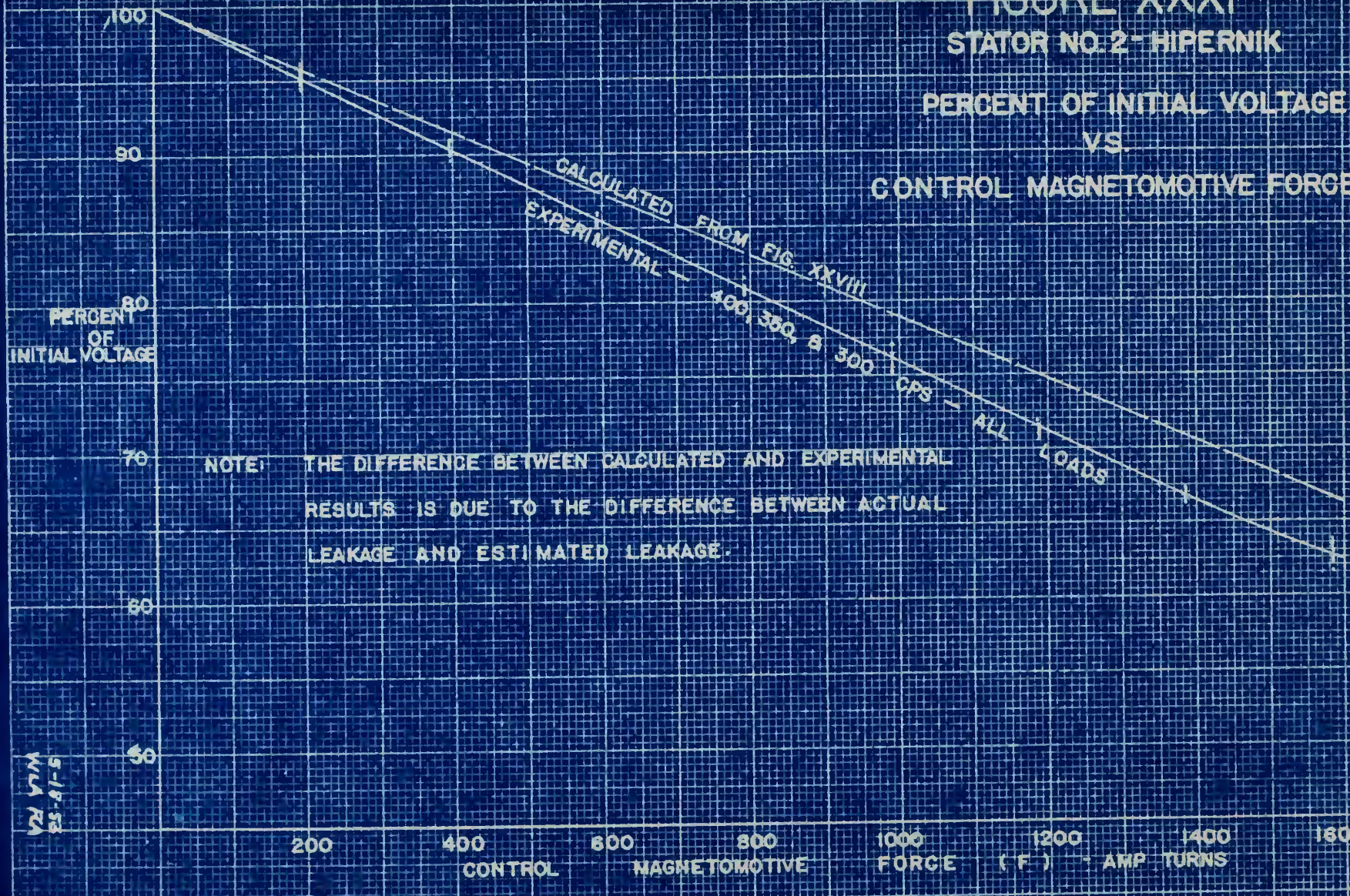

FIGURE XXXI

S-1-8-53 WLM RM

FIGURE XXXII

STATOR NO. 2 - HIPERNIK

PERCENT OF INITIAL VOLTAGE VS. CONTROL MMF FOR VARIOUS LEAKAGE CONDITIONS

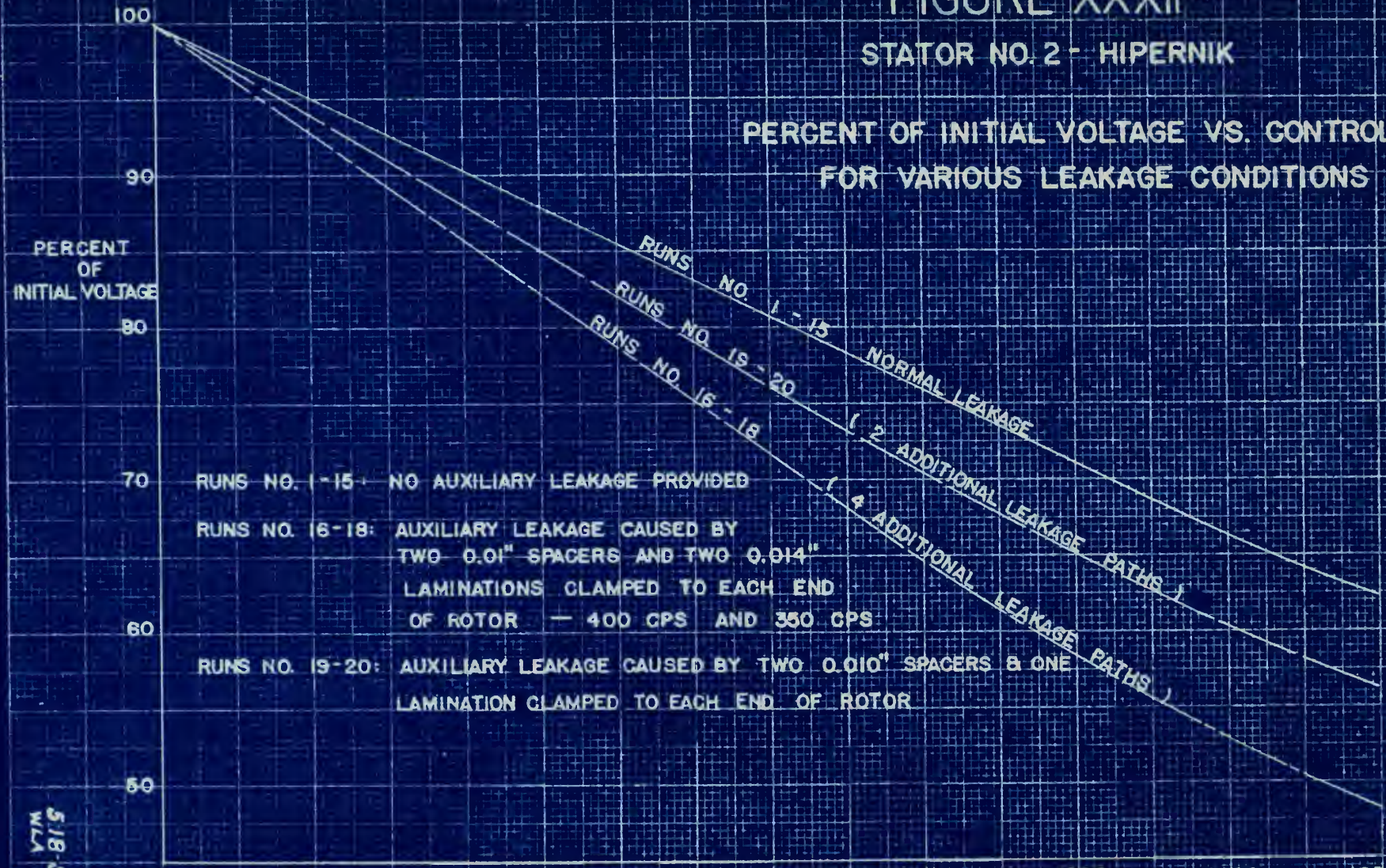

FIGURE XXXII

5-18-53 WLA FCR

SUMMARY OF DATA AND CALCULATIONS (cont.)

Figures XXXIII through XXXVIII:

These curves are all derived from the three curves mentioned on the previous page. They are presented as an aid in visualizing the behavior of the alternator under the specified conditions.

Figures XXVII through XXXVII:

These curves are all derived from the three curves described on the previous page. They are presented as an aid in visualizing the behavior of the alternator under the specified conditions.

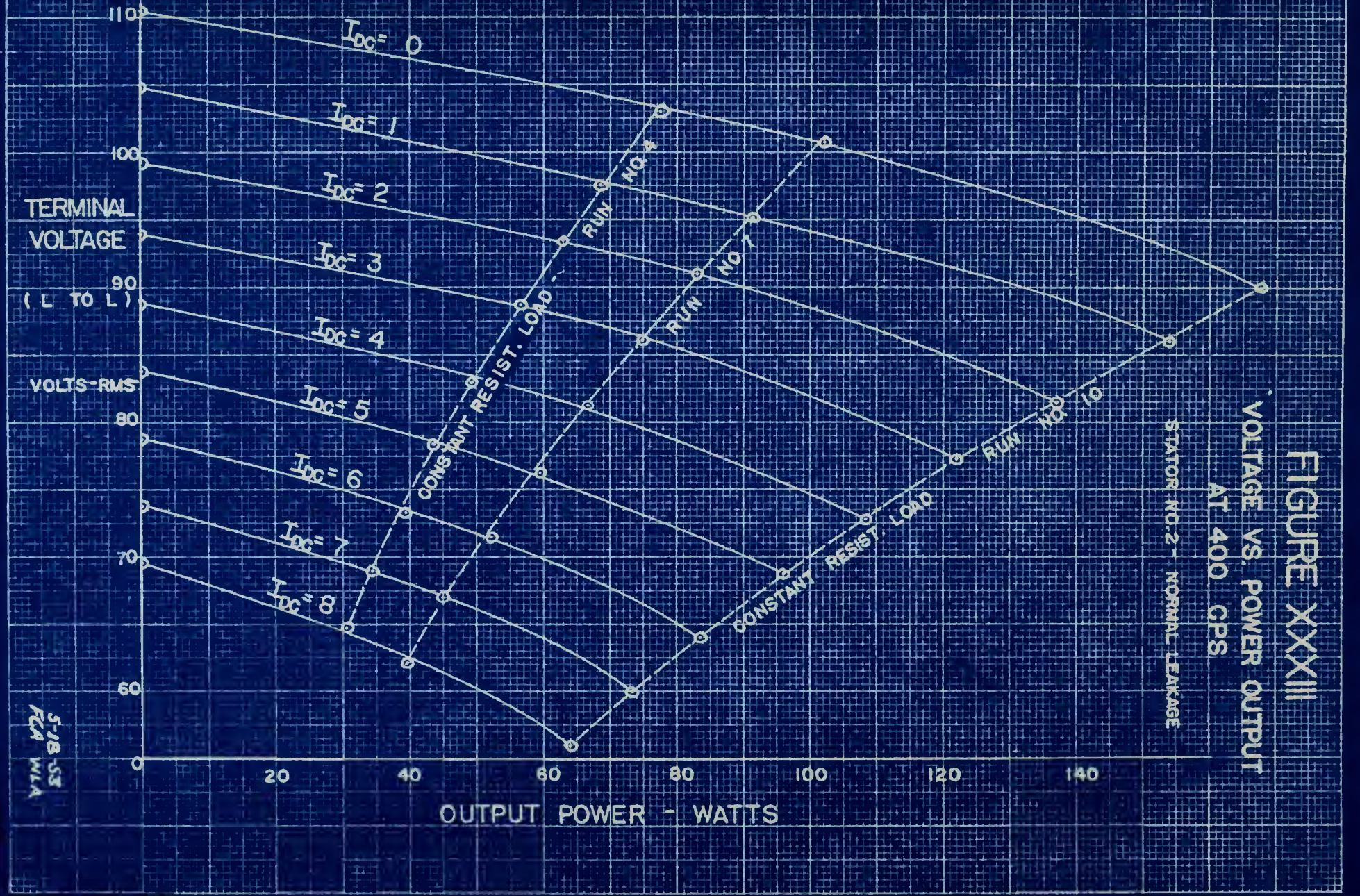
TERMINAL VOLTAGE (L TO L) VOLTS-RMS
110
100
90
80
70
60
0
20
40
60
80
100
120
140
OUTPUT POWER - WATTS
I_{DC}= 0
I_{DC}= 1
I_{DC}= 2
I_{DC}= 3
I_{DC}= 4
I_{DC}= 5
I_{DC}= 6
I_{DC}= 7
I_{DC}= 8
CONSTANT RESIST. LOAD
RUN NO. 4
RUN NO. 7
RUN NO. 10
CONSTANT RESIST. LOAD
STATOR NO. 2 - NORMAL LEAKAGE
FIGURE XXXIII
VOLTAGE VS. POWER OUTPUT AT 400 CPS
5-18-53 FCM W.I.A.

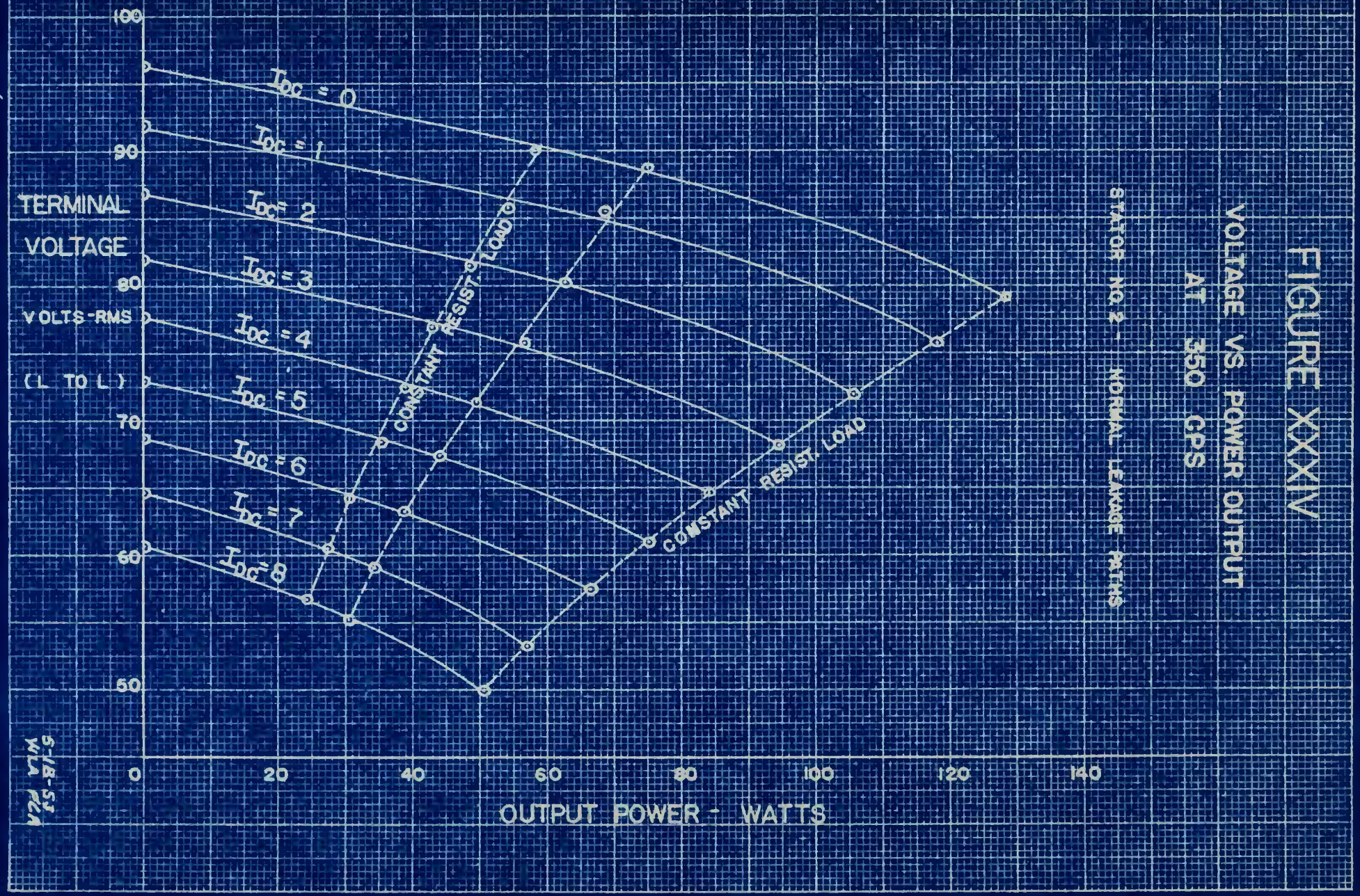
FIGURE XXXIV
VOLTAGE VS. POWER OUTPUT
AT 350 CPS
STATOR NO. 2 - NORMAL LEAKAGE PATHS
TERMINAL VOLTAGE
VOLTS-RMS (L TO L)
100
90
80
70
60
50
0
20
40
60
80
100
120
140
OUTPUT POWER - WATTS
Idc = 0
Idc = 1
Idc = 2
Idc = 3
Idc = 4
Idc = 5
Idc = 6
Idc = 7
Idc = 8
CONSTANT RESIST. LOAD
CONSTANT RESIST. LOAD
9-18-51
W.L.A. Rev.

FIGURE XXXV

VOLTAGE VS. POWER OUTPUT AT 300 CPS

STATOR NO. 2 - NORMAL LEAKAGE PATHS

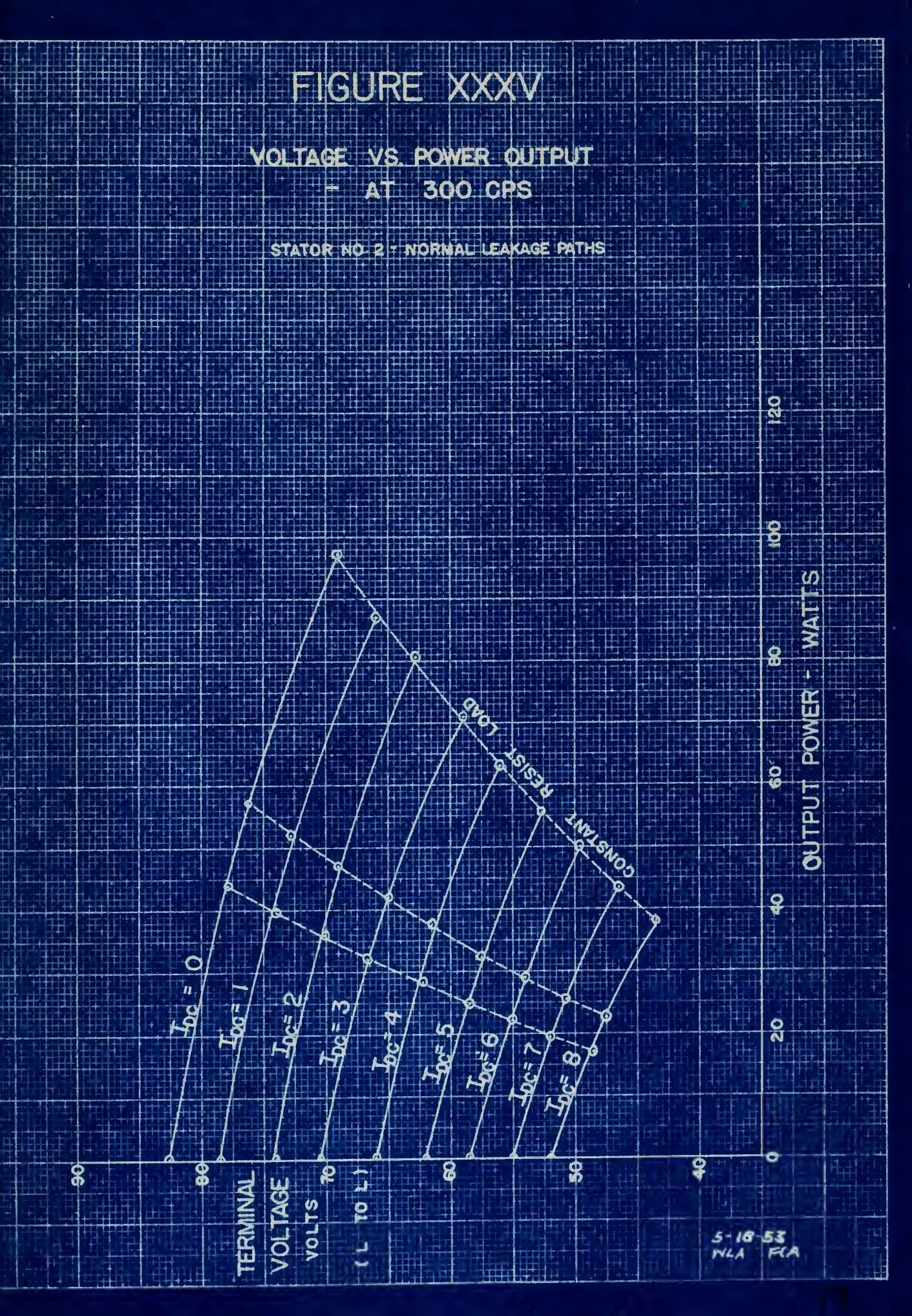

FIGURE XXXVI

POWER ANALYSIS -

USING RECTIFIED OUTPUT POWER FOR CONTROL
TO MAINTAIN CONSTANT VOLTAGE
STATOR NO 2 - 400 CPS - NORMAL LEAKAGE PATHS

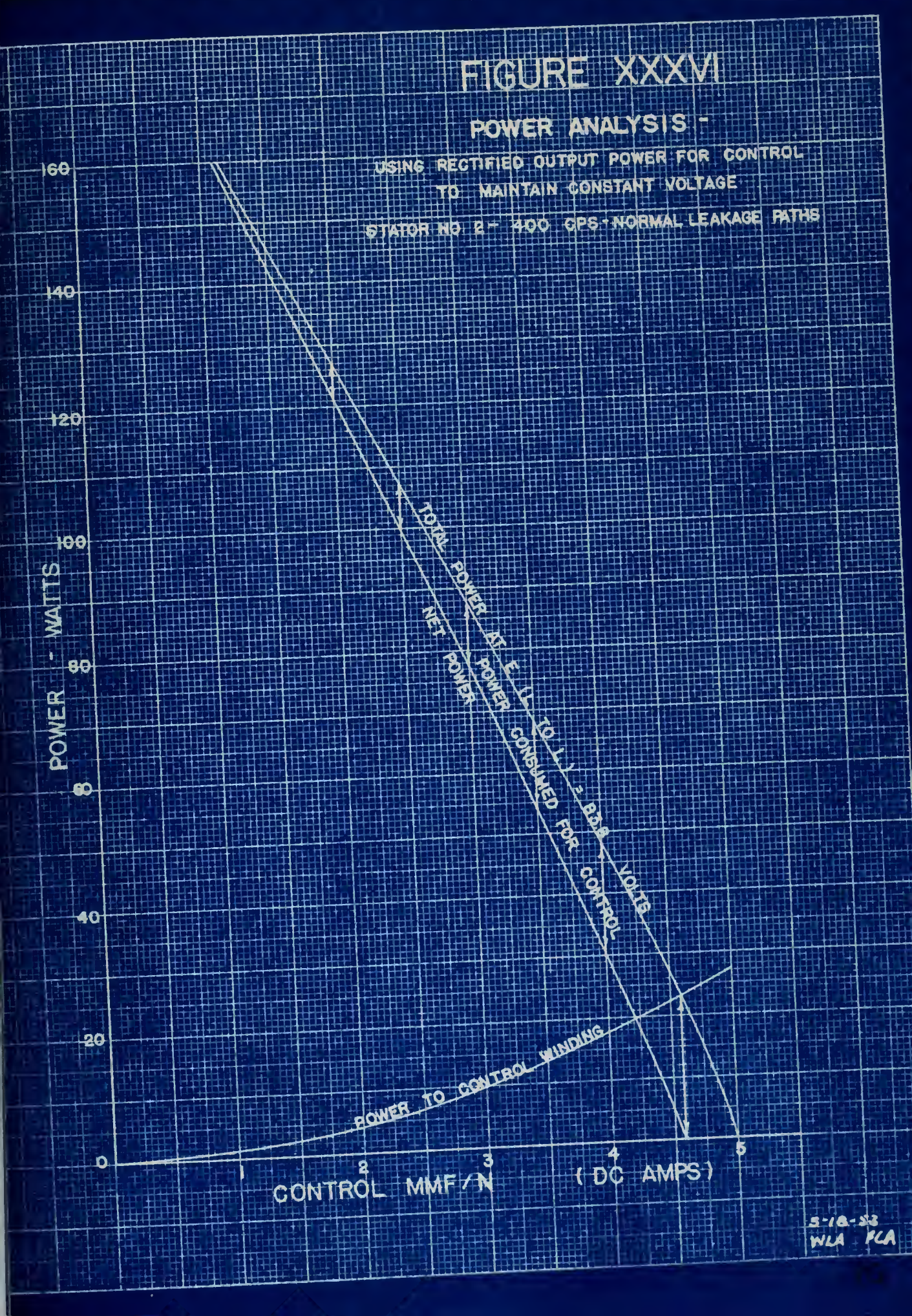

FIGURE XXXVII

CONSTANT POWER OUTPUT WITH VARIABLE ALTERNATOR SPEEDS

BETWEEN 9000 AND 12000 REV. PER MIN.

STATOR NO. 2 - NORMAL LEAKAGE

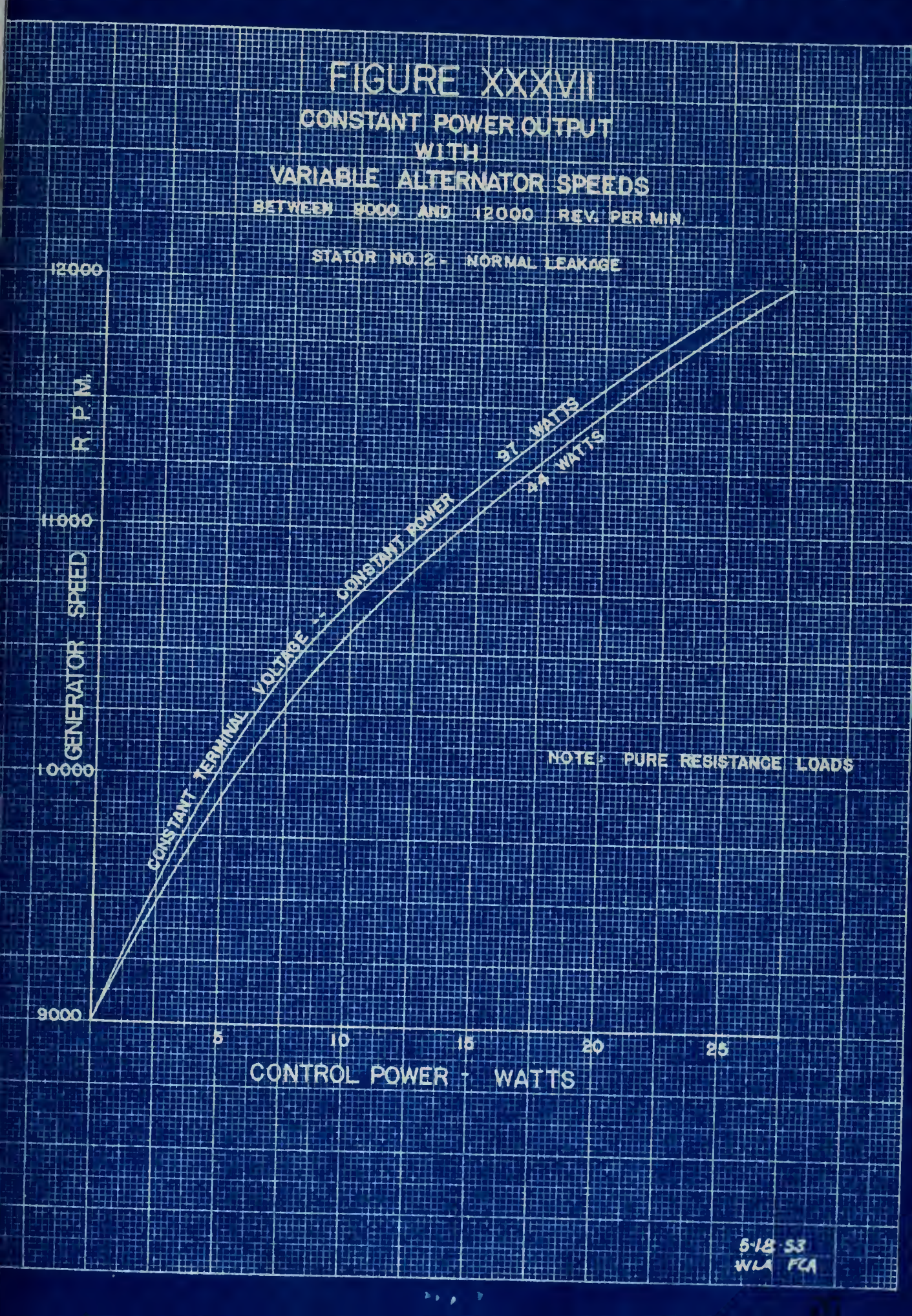

5-18-53
WLA FCA

FIGURE XXXVIII

GENERATOR SPEED VS. CONTROL CURRENT AT CONSTANT TERMINAL VOLTAGE

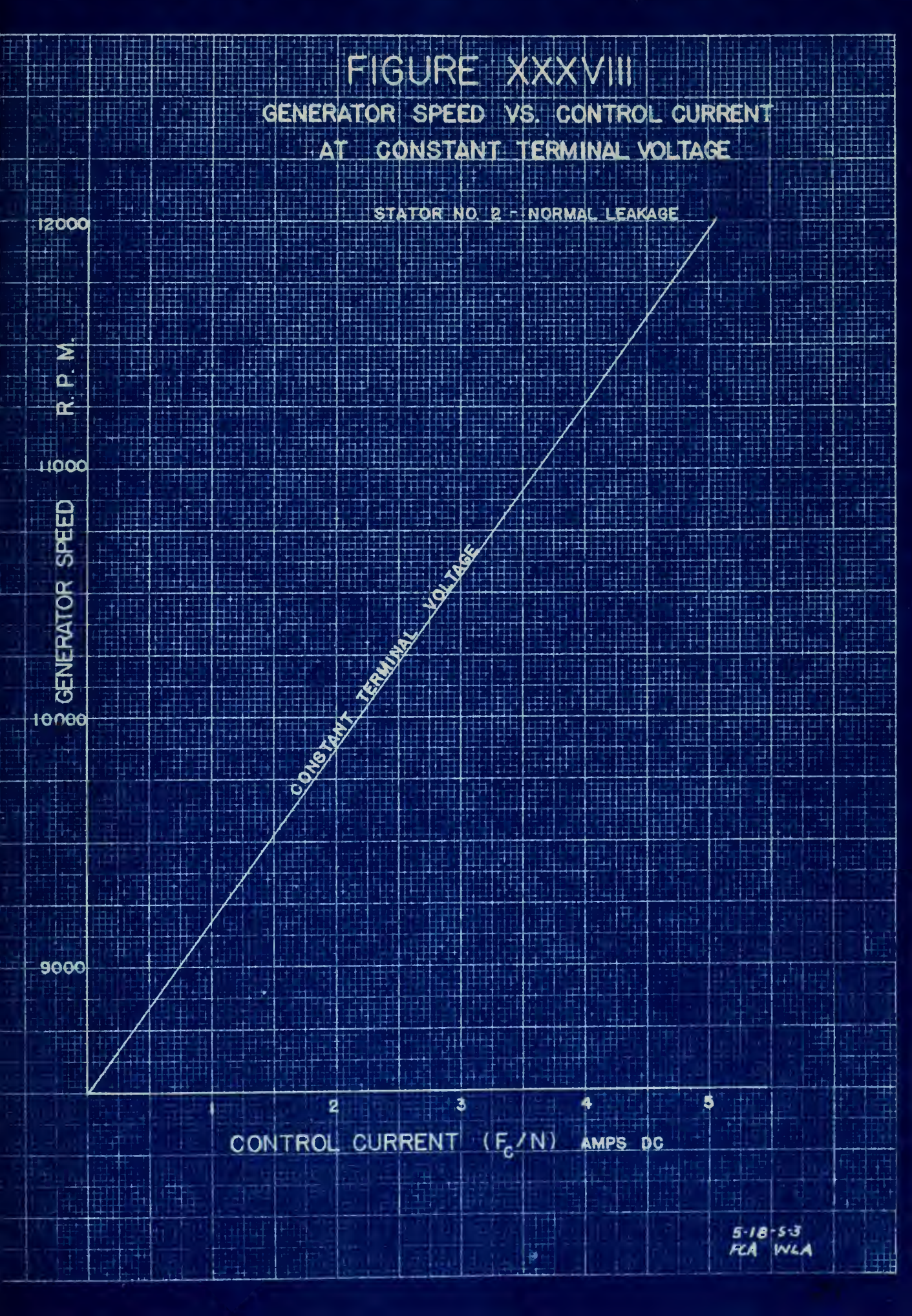

VII. APPENDIX D

EXPERIMENTAL DATA

DATA

STATOR NO. 1
USS ELECTRICAL GRADE STEEL

RUN NO. 1
NO LOAD- CONSTANT FREQUENCY
400 cps

I_{dc} AMPS	F_c AMP-TURNS	$V_{L\ to\ L}$ VOLTS	I_a AMPS	P_{dc} WATTS	P_{ac} WATTS	PERCENT INITIAL V %
0	0	101.5	0	0	No load	100
1	162	99.0	0	0.96	0	97.5
2	324	96.0	0	3.84	0	94.5
3	486	93.0	0	8.64	0	91.5
4	648	89.9	0	15.36	0	88.5
5	810	86.8	0	24.0	0	85.5
6	972	83.9	0	34.56	0	82.6
7	1134	81.0	0	47.04	0	79.7
8	1296	78.1	0	61.44	0	76.9
		RMS				

DATA

STATOR NO. 1
USS ELECTRICAL GRADE STEEL

RUN NO. 2
BALANCED RESISTIVE LOAD—200 OHMS PER PH.
CONSTANT FREQUENCY— 400 cps

I_{dc}	F_c	$V_{L\ to\ L}$	I_a	P_{dc}	P_{ac}	PERCENT INTTIAL V
Amps	Amp-turns	Volts	amps	Watts	Watts	%
0	0	95.0	.2665	0	42.6	100
1	162	92.9	.260	0.96	40.6	97.6
2	324	90.1	.252	3.84	38.1	94.7
3	486	87.1	.244	8.64	35.7	91.6
4	648	83.9	.236	15.36	33.4	88.2
5	810	81.1	.228	24.0	31.2	85.3
6	972	78.1	.219	34.56	28.8	82.1
7	1134	75.4	.211	47.04	26.7	79.3
8	1296	73.0	.205	61.44	25.2	76.75

DATA

STATOR NO. 1
USS ELECTRICAL GRADE STEEL

RUN NO. 3

BALANCED RESISTIVE LOAD - 150 OHMS/PHASE
CONSTANT FREQUENCY - 400 cps

I_{dc}	F_c	$V_{L\ to\ L}$	I_a	P_c	P_{ac}	PERCENT INITIAL V
Amps	Amp-turns	Volts	amps	watts	watts	%
0	0	92.6	.325	0	47.5	100
1	162	90.5	.317	0.96	45.3	97.6
2	324	87.9	.308	3.84	42.6	94.9
3	486	84.9	.298	8.64	40.0	91.6
4	648	82.0	.288	15.36	37.3	88.5
5	810	79.1	.279	24.0	35.0	85.4
6	972	76.5	.269	34.56	32.5	82.6
7	1134	73.6	.259	47.04	30.2	79.4
8	1296	71.0	.251	61.44	28.4	76.7

DATA

STATOR NO. 1
USS ELECTRICAL GRADE STEEL

RUN NO. 4

BALANCED RESISTIVE LOAD - 100 OHMS/PH
CONSTANT FREQUENCY - 400 cps

I_{dc} Amps	F_c Amp-turns	$V_{L\ to\ L}$ Volts	I_a Amps	P_{dc} Watts	P_{ac} Watts	PERCENT INITIAL V %
0	0	89.0	.454	0	61.9	100
1	162	87.1	.444	0.96	59.1	97.9
2	324	84.1	.429	3.84	55.3	94.5
3	486	81.1	.415	8.64	51.8	91.1
4	648	77.6	.398	15.36	47.5	87.2
5	810	74.4	.386	24.00	44.7	83.6
6	972	73.1	.376	34.56	42.4	82.1
7	1134	70.9	.363	47.04	39.5	79.7
8	1296	68.1	.350	61.44	36.8	76.6

DATA

STATOR NO. 1
USS ELECTRICAL GRADE STEEL

RUN NO. 5

BALANCED INDUCTIVE LOAD- 100 OHMS & 100 Mh/PH
CONSTANT FREQUENCY - 400 cps

I_{dc} Amps	F_c Amp-turns	$V_{L\ to\ L}$ Volts	I_a Amps	P_{dc} Watts	P_{ac} Watts	PERCENT INITIAL V %
0	0	93.5	.195	0	11.4	100
1	162	91.2	.191	0.96	10.95	97.5
2	324	88.8	.185	3.84	10.28	95.0
3	486	85.4	.179	8.64	9.62	91.4
4	648	82.8	.174	15.36	9.08	88.6
5	810	80.0	.1675	24.0	8.42	85.6
6	972	77.3	.161	34.56	7.78	82.7
7	1134	74.5	.156	47.04	7.30	79.6
8	1296	72.0	.150	61.44	6.75	77.0

DATA

STATOR NO. 2
HIPERNIK

RUN NO. 1

NO LOAD—CONSTANT FREQUENCY

400 cps

I_{dc}	F_c	$V_{L\ to\ L}$	I_a	P_{dc}	P_{ac}	Percent Initial V
Amps	Amp-turns	Volts	amps	watts	watts	%
0	0	110.5	0	0	0	100
1	198	104.5	0	1.1	0	94.8
2	396	99.3	0	4.4	0	89.8
3	594	94.0	0	10.0	0	85.0
4	792	88.9	0	17.8	0	80.4
5	990	83.8	0	27.7	0	75.8
6	1188	78.8	0	39.5	0	71.4
7	138.6	73.8	0	54.4	0	66.8
8	1584	69.6	0	71.1	0	63.0
		RMS				

DATA

STATOR NO. 2
HIPERNIK

RUN NO. 2

NO LOAD
CONSTANT FREQUENCY - 350 cps

I_{dc} Amps	F_c Amp-turns	$V_{L\ to\ L}$ Volts	I_a Amps	P_{dc} Watts	P_{ac} Watts	PERCENT INITIAL V %
0	0	96.4	0	0	0	100
1	198	92.0	0	1.1	0	95.5
2	396	86.8	0	4.4	0	90.2
3	594	82.0	0	10.0	0	85.2
4	792	77.7	0	17.8	0	80.6
5	990	73.0	0	27.7	0	75.8
6	1188	68.8	0	39.5	0	71.4
7	1386	64.7	0	54.4	0	67.2
8	1584	60.7	0	71.1	0	63.0

DATA

STATOR NO. 2
HIPERNIK

RUN NO. 3

NO LOAD
CONSTANT FREQUENCY - 300 cps

I_{dc} Amps	F_c Amp-turns	$V_{L \text{ to } L}$ Volts	I_a Amps	P_{dc} Watts	P_{ac} Watts	PERCENT INITIAL V %
0	0	82.6	0	0	0	100
1	198	78.5	0	1.1	0	95.0
2	396	74.0	0	4.4	0	89.6
3	594	70.5	0	10.0	0	85.4
4	792	66.0	0	17.8	0	79.8
5	990	62.1	0	27.7	0	75.2
6	1188	58.5	0	39.5	0	70.8
7	1386	55.0	0	54.4	0	66.6
8	1584	52.0	0	71.1	0	63.0

DATA

STATOR NO. 2
HIPERNIK

RUN NO. 4

BALANCED RESISTIVE LOAD - 139.5 OHMS/PH
CONSTANT FREQUENCY - 400 cps

I_{dc}	F_c	$V_{L\ to\ L}$	I_a	P_{dc}	P_{ac}	PERCENT INITIAL V
Amps	Amp-turns	Volts	Amps	Watts	Watts	%
0	0	103	.43	0	77.4	100
1	198	97.5	.405	1.1	68.6	94.6
2	396	93.5	.388	4.4	62.9	90.8
3	594	88.7	.368	10.0	56.6	86.1
4	792	82.9	.343	17.8	49.2	80.6
5	990	78.4	.322	27.7	43.4	76.1
6	1188	73.3	.307	39.5	39.4	71.2
7	1386	69.0	.287	54.4	34.4	67.0
8	1584	64.8	.270	71.1	30.5	62.9

DATA

STATOR NO. 2
HIPERNIK

RUN NO. 5

BALANCED RESISTANCE LOAD - 139.5 OHMS/PH
CONSTANT FREQUENCY - 350 cps

I_{dc} Amps	F_c Amp-Turn	$V_{L\ to\ L}$ Volts	I_a Amps	P_{dc} Watts	P_{ac} Watts	PERCENT INITIAL V %
0	0	90.0	.372	0	57.9	100
1	198	85.8	.360	1.1	54.2	95.4
2	396	81.5	.340	4.4	48.4	90.6
3	594	77.0	.320	10.0	42.9	85.6
4	792	72.5	.305	17.8	39.0	80.6
5	990	68.5	.290	27.7	35.2	76.1
6	1188	64.3	.270	39.5	30.5	71.5
7	1386	60.5	.255	54.4	27.2	67.2
8	1584	56.8	.240	71.1	24.1	63.2

DATA

STATOR NO. 2
HIPERNIK

RUN NO. 6

BALANCED RESISTIVE LOAD - 139.5 OHMS/PH
CONSTANT FREQUENCY - 300 cps

I_{dc} Amps	F_c Amp-turns	$V_{L\ to\ L}$ Volts	I_a Amps	P_{dc} Watts	P_{ac} Watts	PERCENT INITIAL V %
0	0	77.9	.324	0	43.9	100
1	198	74.0	.308	1.1	39.7	95.0
2	396	70.1	.293	4.4	35.9	90.0
3	594	66.7	.277	10.0	32.1	85.6
4	792	62.2	.260	17.8	28.3	79.8
5	990	58.5	.244	27.7	24.9	75.1
6	1188	55.0	.230	39.5	22.2	70.6
7	1386	52.0	.215	54.4	19.4	66.8
8	1584	48.5	.201	71.1	16.9	62.3

DATA

STATOR NO. 2
HIPERNIK

RUN NO. 7

BALANCED RESISTIVE LOAD - 93 OHMS/PH
CONSTANT FREQUENCY - 400 cps

I_{dc} Amps	F_c Amp-turns	$V_{L\ to\ L}$ Volts	I_a Amps	P_{dc} Watts	P_{ac} Watts	PERCENT INITIAL V %
0	0	100.8	.605	0	102.1	100
1	198	95.1	.572	1.1	91.3	94.4
2	396	91.0	.545	4.4	82.9	90.3
3	594	86.1	.518	10.0	74.9	85.5
4	792	81.2	.489	17.8	66.7	80.5
5	990	76.2	.462	27.7	59.5	75.6
6	1188	71.5	.432	39.5	52.0	70.9
7	1386	67.0	.401	54.4	44.9	66.5
8	1584	62.1	.376	71.1	39.5	61.6

DATA

STATOR NO. 2
HIPERNIK

RUN NO. 8

BALANCED RESISTIVE LOAD - 93 OHMS/PH
CONSTANT FREQUENCY - 350 cps

I_{dc} Amps	F_c Amp-turns	$V_{L\ to\ L}$ Volts	I_a Amps	P_{dc} Watts	P_{ac} Watts	PERCENT INITIAL V %
0	0	88.8	.518	0	74.9	100
1	198	85.5	.496	1.1	68.6	96.2
2	396	80.2	.472	4.4	62.6	90.2
3	594	75.8	.450	10.0	56.5	85.3
4	792	71.4	.421	17.8	49.5	80.1
5	990	67.4	.397	27.7	43.9	75.8
6	1188	63.3	.373	39.5	38.8	71.3
7	1386	59.1	.350	54.4	34.2	66.5
8	1584	55.2	.330	71.1	30.4	62.1

DATA

STATOR NO. 2
HIPERNIK

RUN NO. 9

BALANCED RESISTIVE LOAD - 93 OHMS/PH
CONSTANT FREQUENCY - 300 cps

I_{dc} Amps	F_c Amp-turns	$V_{L\ to\ L}$ Volts	I_a Amps	P_{dc} Watts	P_{ac} Watts	PERCENT INITIAL V %
0	0	76.2	.453	0	57.2	100
1	198	72.8	.432	1.1	52.0	95.8
2	396	69.0	.410	4.4	46.9	90.6
3	594	65.0	.388	10.0	42.0	85.4
4	792	61.5	.367	17.9	37.6	80.9
5	990	57.5	.340	27.7	32.2	75.6
6	1188	54.0	.322	39.5	28.9	70.9
7	1386	50.7	.302	54.4	25.4	66.6
8	1584	47.5	.285	71.1	22.6	62.4

DATA

STATOR NO. 2
HIPERNIK

RUN NO. 10

BALANCED RESISTIVE LOAD - 46.5 OHMS/PH
CONSTANT FREQUENCY - 400 cps

I_{dc} Amps	F_c Amp-turns	$V_{L\ to\ L}$ Volts	I_a Amps	P_{dc} Watts	P_{ac} Watts	PERCENT INITIAL V %
0	0	90.0	1.097	0	167.8	100
1	198	86.0	1.05	1.1	153.9	95.6
2	396	81.5	0.99*	4.4	136.9	90.6
3	594	77.3	0.935	10.0	122.0	85.9
4	792	72.8	0.882	17.8	108.5	81.0
5	990	68.8	0.830	27.7	96.1	76.5
6	1188	64.0	0.772	39.5	83.3	71.2
7	1386	60.0	0.725	54.4	73.4	66.7
8	1584	56.0	0.677	71.1	63.9	62.2

* CHANGE IN AMMETERS WAS REQUIRED

DATA

STATOR NO. 2
HIPERNIK

RUN NO. 11

BALANCED RESISTIVE LOAD - 46.5 OHMS/PH
CONSTANT FREQUENCY - 350 cps

I_{dc} Amps	F_c Amp-turns	$V_{L\ to\ L}$ Volts	I_a Amps	P_{dc} Watts	P_{ac} Watts	PERCENT INITIAL V %
0	0	79.1	.957	0	128.2	100
1	198	75.7	.920	1.1	118.1	95.6
2	396	72.0	.870	4.4	105.7	90.9
3	594	68.2	.824	10.0	94.6	86.1
4	792	64.4	.776	17.8	84.1	81.6
5	990	61.0	.734	27.7	75.1	77.1
6	1188	57.5	.690	39.5	66.4	72.6
7	1386	53.2	.640	54.4	57.1	67.2
8	1584	50.0	.601	71.1	50.4	63.1

DATA

STATOR NO. 2
HIPERNIK

RUN NO. 12

BALANCED RESISTIVE LOAD - 46.5 OHMS/PH
CONSTANT FREQUENCY - 300 cps

I_{dc} Amps	F_c Amp-turns	$V_{L\ to\ L}$ Volts	I_a Amps	P_{dc} Watts	P_{ac} Watts	PERCENT INITIAL V %
0	0	69.1	.835	0	97.3	100
1	198	66.0	.79	1.1	87.0	95.5
2	396	62.8	.76	4.4	80.6	91.0
3	594	59.0	.713	10.0	70.9	85.4
4	792	56.0	.673	17.8	63.1	81.0
5	990	52.7	.632	27.7	55.7	76.2
6	1188	49.6	.598	39.5	49.9	71.8
7	1386	46.5	.558	54.4	43.4	67.3
8	1584	43.5	.521	71.1	37.9	62.9

DATA

STATOR NO. 2
HIPERNIK

RUN NO. 13

BALANCED INDUCTIVE LOAD- 100 OHMS & 100 MILLIHENRIES/PH
CONSTANT FREQUENCY - 400 cps

I_{dc} Amps	F_c Amp-turns	$V_{L\ to\ L}$ Volts	I_a Amps	P_{dc} Watts	P_{ac} Watts	PERCENT INITIAL V %
0	0	102.5	.215	0	13.9	100
1	198	97.5	.204	1.1	12.5	95.1
2	396	92.5	.194	4.4	11.3	90.2
3	594	87.5	.183	10.0	10.0	85.3
4	792	82.5	.172	17.8	8.87	80.5
5	990	78.0	.163	27.7	8.02	76.1
6	1188	73.0	.153	39.5	7.03	71.2
7	1386	69.0	.144	54.4	62.1	67.3
8	1584	65.0	.135	71.1	5.47	63.4

DATA

STATOR NO. 2
HIPERNIK

RUN NO. 14

BALANCED INDUCTIVE LOAD - 100 OHMS & 100 MILLIHENRIES/PH
CONSTANT FREQUENCY - 350 cps

I_{dc} Amps	F_c Amp-turns	$V_{L\ to\ L}$ Volts	I_a Amps	P_{dc} Watts	P_{ac} Watts	PERCENT INITIAL V %
0	0	89.0	.206	0	12.7	100
1	198	84.8	.196	1.1	11.5	95.3
2	396	80.5	.186	4.4	10.4	90.5
3	594	76.0	.176	10.0	9.29	85.4
4	792	71.8	.165	17.8	8.17	80.75
5	990	67.0	.156	27.7	7.30	75.3
6	1188	64.0	.147	39.5	6.49	71.9
7	1386	60.0	.136	54.4	5.55	67.4
8	1584	56.5	.130	71.1	5.08	63.5

DATA

STATOR NO. 2
HIPERNIK

RUN NO. 15

BALANCED INDUCTIVE LOAD - 100 OHMS & 100 MILLIHENRIES/PH
CONSTANT FREQUENCY - 300 cps

I_{dc} Amps	F_c Amp-turns	$V_{L\ to\ L}$ Volts	I_a Amps	P_{dc} Watts	P_{ac} Watts	PERCENT INITIAL V %
0	0	76.5	.201	0	12.1	100
1	198	72.7	.190	1.1	10.8	95.1
2	396	69.0	.181	4.4	9.83	90.3
3	594	65.1	.171	10.0	8.79	85.1
4	792	61.8	.161	17.8	7.77	80.9
5	990	58.0	.151	27.7	6.84	75.8
6	1188	54.8	.141	39.5	5.96	71.8
7	1386	51.5	.134	54.4	5.39	67.3
8	1584	48.8	.125	71.1	4.69	63.8

DATA

STATOR NO. 2
HIPERNIK

RUN NO. 16

EFFECTS OF INCREASED LEAKAGE:

TWO 0.010" TEFLON SPACERS PLUS TWO 0.014"
HIPERNIK LAMINATIONS CLAMPED TO EACH END OF ROTOR

NO LOAD
CONSTANT FREQUENCY - 400 cps

I_{dc} Amps	F_c Amp-turns	$V_{L\ to\ L}$ Volts	I_a Amps	P_{dc} Watts	P_{ac} Watts	PERCENT INITIAL V %
0	0	89.5	0	0	0	100
1	198	82.8	0	1.1	0	92.5
2	396	76.0	0	4.4	0	84.8
3	594	69.7	0	10.0	0	77.8
4	792	63.6	0	17.8	0	71.0
5	990	58.0	0	27.7	0	64.75
6	1188	52.7	0	39.5	0	58.8
7	1386	48.0	0	54.4	0	53.6
8	1584	43.5	0	71.1	0	48.6

DATA

STATOR NO. 2
HIPERNIK

RUN NO. 17

EFFECTS OF INCREASED LEAKAGE:

TWO 0.010" TEFLON SPACERS PLUS TWO 0.014" HIPERNIK LAMINATIONS CLAMPED TO EACH END OF THE ROTOR

BALANCED RESISTIVE LOAD - 100 OHMS/PH
CONSTANT FREQUENCY - 400 cps

I_{dc} Amps	F_c Amp-turns	$V_{L\ to\ L}$ Volts	I_a Amps	P_{dc} Watts	P_{ac} Watts	PERCENT INITIAL V %
0	0	80.5	.427	0	54.8	100
1	198	75.0	.400	1.1	48.0	93.2
2	396	69.1	.367	4.4	40.4	85.8
3	594	63.1	.332	10.0	33.1	78.4
4	792	57.8	.306	17.8	28.1	71.9
5	990	52.6	.280	27.7	23.6	65.3
6	1188	47.5	.254	39.5	19.4	59.0
7	1386	42.9	.228	54.4	15.6	53.3
8	1584	39.0	.206	71.1	12.7	48.4

DATA

STATOR NO. 2
HIPERNIK

RUN NO. 18

EFFECTS OF INCREASED LEAKAGE:

TWO 0.010" TEFLON SPACERS PLUS TWO 0.014" HIPERNIK LAMINATIONS CLAMPED TO EACH END OF ROTOR

BALANCED RESISTIVE LOAD - 100 OHMS/PH
CONSTANT FREQUENCY - 350 cps

I_{dc} Amps	F_c Amp-turns	$V_{L\ to\ L}$ Volts	I_a Amps	P_{dc} Watts	P_{ac} Watts	PERCENT INITIAL V %
0	0	70.0	.375	0	42.2	100
1	198	65.1	.351	1.1	37.0	93.1
2	396	59.8	.322	4.4	31.1	85.5
3	594	55.1	.296	10.0	26.3	78.8
4	792	50.2	.270	17.8	21.9	71.8
5	990	45.5	.246	27.7	18.2	65.0
6	1188	41.5	.223	39.5	14.9	59.4
7	1386	37.5	.200	54.4	12.0	53.6
8	1584	34.0	.180	71.1	9.73	48.6

DATA

STATOR NO. 2
HIPERNIK

RUN NO. 19

EFFECTS OF INCREASED LEAKAGE:

TWO 0.010" TEFLON SPACERS PLUS ONE 0.014" HIPERNIK LAMINATION CLAMPED TO EACH END OF ROTOR

NO LOAD
CONSTANT FREQUENCY - 400 cps

I_{dc} Amps	F_c Amp-turns	$V_{L\ to\ L}$ Volts	I_a Amps	P_{dc} Watts	P_{ac} Watts	PERCENT INITIAL V %
0	0	97	0	0	0	100
1	198	91.3	0	1.1	0	94.2
2	396	85.5	0	4.4	0	88.2
3	594	79.6	0	10.0	0	82.1
4	792	73.9	0	17.8	0	76.3
5	990	69.0	0	27.7	0	71.2
6	1188	63.8	0	39.5	0	65.8
7	1386	59.0	0	54.4	0	60.9
8	1584	54.9	0	71.1	0	56.6

DATA

STATOR NO. 2
HIPERNIK

RUN NO. 20

EFFECTS OF INCREASED LEAKAGE:

TWO 0.010" TEFLON SPACERS PLUS ONE 0.014" HIPERNIK
LAMINATION CLAMPED TO EACH END OF ROTOR

BALANCED RESISTIVE LOAD - 100 OHMS/PH
CONSTANT FREQUENCY - 400 cps

I_{dc}	F_c	$V_{L\ to\ L}$	I_a	P_{dc}	P_{ac}	PERCENT INITIAL V
Amps	Amp-turns	Volts	Amps	Watts	Watts	%
0	0	88.5	.468	0	65.8	100
1	198	83.2	.442	1.1	58.7	94.1
2	396	78.1	.415	4.4	51.8	88.3
3	594	72.8	.388	10.0	45.2	82.3
4	792	68.0	.362	17.8	39.4	76.9
5	990	63.1	.336	27.7	33.9	71.3
6	1188	58.4	.310	39.5	28.8	66.0
7	1386	53.8	.288	54.4	24.9	60.8
8	1584	50.0	.266	71.1	21.2	56.5

BIBLIOGRAPHY

1 H. C. Roters; "Electromagnetic Devices", John Wiley & Sons, 1951 pp. 84-115.

2 C. T. Thomas and J. R. Ireland; "The Design and Performance of Permanent Magnet Rotors" - Elec. Mfg. Aug. 1947, p. 110.

3 K. L. Scott; "Magnet Steels and Permanent Magnets", AIEE Trans., Vol. 51, 1932, p. 410.

4 Indiana Steel Co.; "Indiana Steel Permanent Magnet Manual No. 4".

5 EE Staff, M.I.T.; "Magnetic Circuits and Transformers", Technology Press, M.I.T., John Wiley & Sons, Inc. pp. 90-93.

6 E. H. Harris; EE Thesis, 1950, M.I.T., "Magnetic Amplifiers with AC Control".

7 O. T. Estes and W. J. Hussong, Nav. Arch. Thesis, 1951, M.I.T.; "Study of Capacitor-Excited Induction Generators; Parallel Operation and Transient Loading".

8 R. W. Goode, H. A. Hoffmann, and W. F. Searle, Jr.; Nav. Arch. Thesis, 1952, M.I.T.; "The Experimental Determination of the Performance of a Capacitor Excited Induction Generator with an Inductive Reactance in Series with the Load".

9 J. H. Kulhman; "Design of Electrical Apparatus". John Wiley & Sons, 1930, pp. 174-214.

BIBLIOGRAPHY

1 H. C. Rogers: "Electromagnetic Devices", Iron Valley & Dome, 1951, pp. 89-145.

2 C. T. Thomas and J. B. Ireland: "The Design and Performance of Permanent Magnet Motors" - Elec. Mfg. Aug. 1947, p. 130.

3 E. L. Scott: "Magnet Steels and Permanent Magnets", AIEE Trans., Vol. 51, 1932, p. 416.

4 Indiana Steel Co.: "Indiana Steel Permanent Magnet Manual No. 4".

5 Ed Scott, M.I.T.: "Magnetic Circuits and Transformers", Technology Press, M.I.T., John Wiley & Sons, Inc. pp. 50-95.

6 H. Harris: Ed Thesis, 1950, M.I.T., "Magnetic Amplifiers with AC Control".

7 O. T. Estes and W. J. Bussard, Rev. Arch. Thesis, 1951, M.I.T.: "Study of Capacitor-Assisted Induction Generators; Parallel Operation and Transient Loading".

8 R. W. Goode, R. A. Moffenden, and W. E. Harris, Jr.: Rev. Arch. Thesis, 1950, M.I.T.: "The Experimental Determination of the Performance of a Capacitive-Excited Induction Generator Operating with an Inductive Reactance in Series with the Load".

9 F. E. Kullmann: "Design of Electrical Apparatus", John Wiley & Sons, 1939, pp. 179-217.

31

a-